





37-1  
National Bureau of Standards  
Library, E-01 Admin. Bldg.  
MAR 28 1970

# NBS TECHNICAL NOTE 514

## ARPA-NBS Program of Research on High Temperature Materials and Laser Materials

UNITED STATES  
DEPARTMENT OF  
COMMERCE  
PUBLICATION



U.S.  
DEPARTMENT  
OF  
COMMERCE

National  
Bureau  
of  
Standards

## NATIONAL BUREAU OF STANDARDS

The National Bureau of Standards<sup>1</sup> was established by an act of Congress March 3, 1901. Today, in addition to serving as the Nation's central measurement laboratory, the Bureau is a principal focal point in the Federal Government for assuring maximum application of the physical and engineering sciences to the advancement of technology in industry and commerce. To this end the Bureau conducts research and provides central national services in four broad program areas. These are: (1) basic measurements and standards, (2) materials measurements and standards, (3) technological measurements and standards, and (4) transfer of technology.

The Bureau comprises the Institute for Basic Standards, the Institute for Materials Research, the Institute for Applied Technology, the Center for Radiation Research, the Center for Computer Sciences and Technology, and the Office for Information Programs.

**THE INSTITUTE FOR BASIC STANDARDS** provides the central basis within the United States of a complete and consistent system of physical measurement; coordinates that system with measurement systems of other nations; and furnishes essential services leading to accurate and uniform physical measurements throughout the Nation's scientific community, industry, and commerce. The Institute consists of an Office of Measurement Services and the following technical divisions:

Applied Mathematics—Electricity—Metrology—Mechanics—Heat—Atomic and Molecular Physics—Radio Physics<sup>2</sup>—Radio Engineering<sup>2</sup>—Time and Frequency<sup>2</sup>—Astrophysics<sup>2</sup>—Cryogenics.<sup>2</sup>

**THE INSTITUTE FOR MATERIALS RESEARCH** conducts materials research leading to improved methods of measurement standards, and data on the properties of well-characterized materials needed by industry, commerce, educational institutions, and Government; develops, produces, and distributes standard reference materials; relates the physical and chemical properties of materials to their behavior and their interaction with their environments; and provides advisory and research services to other Government agencies. The Institute consists of an Office of Standard Reference Materials and the following divisions:

Analytical Chemistry—Polymers—Metallurgy—Inorganic Materials—Physical Chemistry.

**THE INSTITUTE FOR APPLIED TECHNOLOGY** provides technical services to promote the use of available technology and to facilitate technological innovation in industry and Government; cooperates with public and private organizations in the development of technological standards, and test methodologies; and provides advisory and research services for Federal, state, and local government agencies. The Institute consists of the following technical divisions and offices:

Engineering Standards—Weights and Measures—Invention and Innovation—Vehicle Systems Research—Product Evaluation—Building Research—Instrument Shops—Measurement Engineering—Electronic Technology—Technical Analysis.

**THE CENTER FOR RADIATION RESEARCH** engages in research, measurement, and application of radiation to the solution of Bureau mission problems and the problems of other agencies and institutions. The Center consists of the following divisions:

Reactor Radiation—Linac Radiation—Nuclear Radiation—Applied Radiation.

**THE CENTER FOR COMPUTER SCIENCES AND TECHNOLOGY** conducts research and provides technical services designed to aid Government agencies in the selection, acquisition, and effective use of automatic data processing equipment; and serves as the principal focus for the development of Federal standards for automatic data processing equipment, techniques, and computer languages. The Center consists of the following offices and divisions:

Information Processing Standards—Computer Information—Computer Services—Systems Development—Information Processing Technology.

**THE OFFICE FOR INFORMATION PROGRAMS** promotes optimum dissemination and accessibility of scientific information generated within NBS and other agencies of the Federal government; promotes the development of the National Standard Reference Data System and a system of information analysis centers dealing with the broader aspects of the National Measurement System, and provides appropriate services to ensure that the NBS staff has optimum accessibility to the scientific information of the world. The Office consists of the following organizational units:

Office of Standard Reference Data—Clearinghouse for Federal Scientific and Technical Information<sup>4</sup>—Office of Technical Information and Publications—Library—Office of Public Information—Office of International Relations.

<sup>1</sup> Headquarters and Laboratories at Gaithersburg, Maryland, unless otherwise noted; mailing address Washington, D.C. 20234.

<sup>2</sup> Located at Boulder, Colorado 80302.

<sup>3</sup> Located at 5285 Port Royal Road, Springfield, Virginia 22151.

UNITED STATES DEPARTMENT OF COMMERCE  
Maurice H. Stans, Secretary  
NATIONAL BUREAU OF STANDARDS • Lewis M. Branscomb, Director



# TECHNICAL NOTE 514

ISSUED JANUARY 1970

Nat. Bur. Stand. (U.S.), Tech. Note 514, 98 pages (Jan. 1970)

CODEN: NBTNA

## **ARPA-NBS Program of Research on High Temperature Materials and Laser Materials**

Reporting Period  
January 1 to June 30, 1969

Edited by A. D. Franklin and H. S. Bennett

Inorganic Materials Division  
Institute for Materials Research  
National Bureau of Standards  
Washington, D.C. 20234

Supported by the  
Advanced Research Projects Agency  
of the Department of Defense

NBS Technical Notes are designed to supplement the Bureau's regular publications program. They provide a means for making available scientific data that are of transient or limited interest. Technical Notes may be listed or referred to in the open literature.

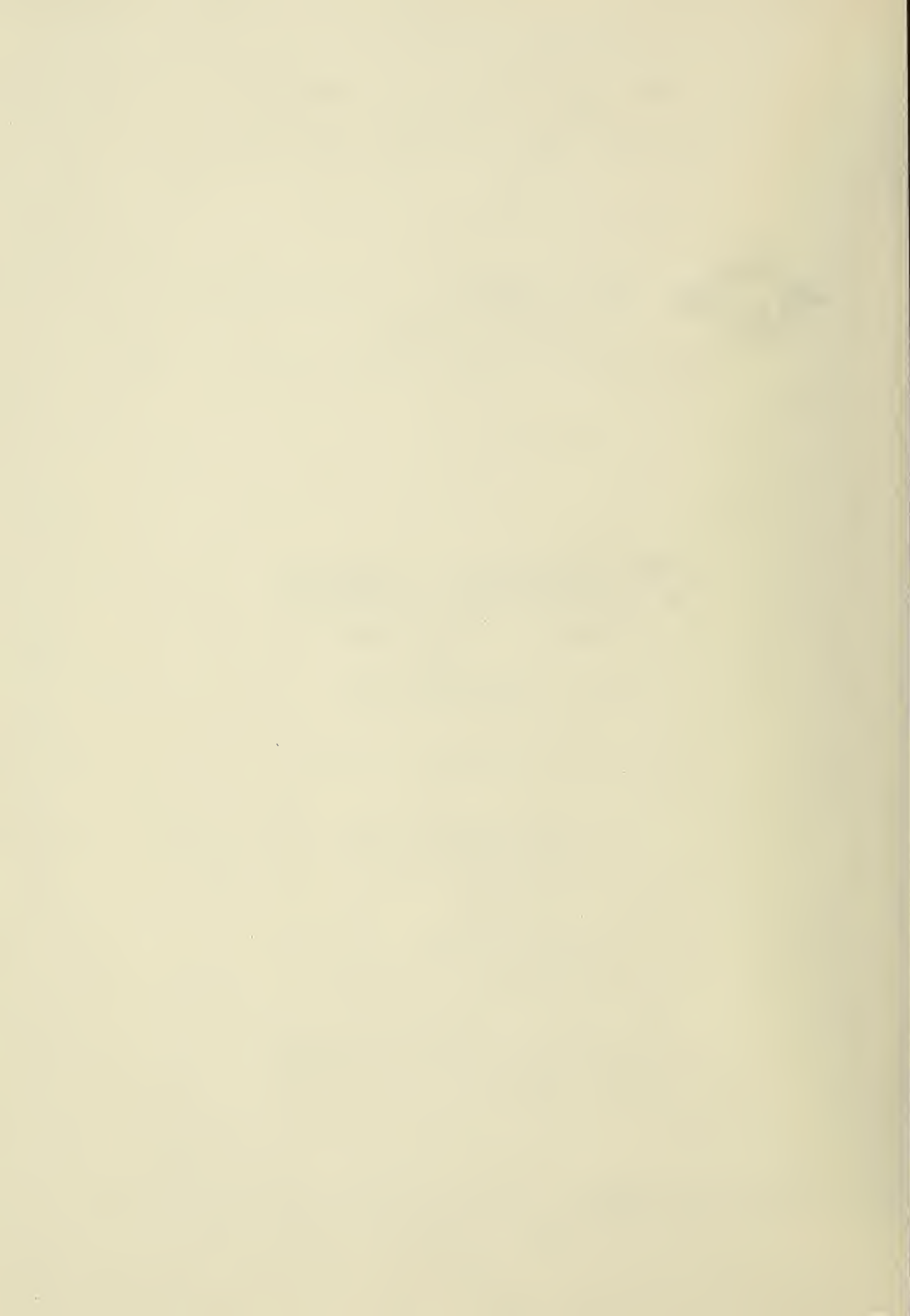


# TABLE OF CONTENTS

	Page
1. Introduction . . . . .	1
2. Objectives . . . . .	1
3. Project Summaries. . . . .	4
3.1. Diffusion in Oxides	
3.1.1. Diffusion in Refractory Materials. . . . .	4
3.1.2. Diffusion of Oxygen in Oxides. . . . .	8
3.1.3. Crystal Growth from Vapor. . . . .	22
3.2. Properties of Refractory Borides	
3.2.1. Electronic Structure of Refractory Hard Metals. . . . .	24
3.3. High Temperature Metals	
3.3.1. Optical Constants of Titanium in the Visible Region of the Spectrum . . . . .	29
3.3.2. High Temperature Creep in Metals . . . . .	31
3.4. Ceramics	
3.4.1. Deformation and Fracture of Ionic Crystals . . . . .	38
3.5. Polymers	
3.5.1. The Volatilization and Decomposition of Materials . . . . .	40
3.5.2. Relaxations Near the Melting Point . . . . .	43
3.6. Laser Materials	
3.6.1. Bulk Properties of Laser Materials . . . . .	44
3.6.2. Crystal Defect Studies on Laser Materials. . . . .	50
3.6.3. Examination of Ruby Laser Rods by X-ray Diffraction Techniques . . . . .	58
3.6.4. Laser Induced Damage Studies . . . . .	62
3.6.5. Characterization Standards for Laser Materials. . . . .	67
3.6.6. Studies on Techniques to Detect Platinum Inclusions and to Measure Nd-Glass Quality by Light Scattering	73
3.6.7. Appendix - Trip Reports. . . . .	75

ARPA-NBS PROGRAM OF RESEARCH ON  
HIGH TEMPERATURE MATERIALS  
AND  
LASER MATERIALS

Work Performed at the National Bureau of Standards  
Supported by the Advanced Research Projects Agency,  
Department of Defense

Reporting Period January 1 - June 30, 1969

Edited by

A. D. Franklin and H. S. Bennett

Brief reviews are given of work performed during the period January 1 to June 30, 1969, on a number of projects concerned with High Temperature Materials and with Laser Materials. Under the High Temperature Materials heading, topics include diffusion of oxygen in oxides, growth of  $Al_2O_3$  crystals by chemical vapor deposition, the electronic structure of transition metal borides and related compounds, the optical constants of titanium, high temperature creep in copper, fracture in glass, the mechanism of volatilization of polymers and long-chain compounds, and the interaction between mechanical relaxation and annealing in polymers. Work on Laser Materials includes measurement of bulk optical and elastic properties of laser materials, a study of the "orange" degradation of ruby, measurements of sub-crystal misalignment in ruby, damage in glass induced by high-energy laser pulses, chemical analyses for ruby and Nd-doped laser glasses, and preliminary studies on detection of submicroscopic inhomogeneities in glass.

Key words: Band structure, chemical analysis, copper, creep, crystal defects, crystal growth, diffusion, evaporation, fracture, glass, high temperature materials, inhomogeneities in glass, laser damage, laser glass, lasers, mass transport, materials properties, mechanical relaxation, metal borides, optical properties, opto-elastic properties, oxides, polymers, ruby, titanium, transition



ARPA-NBS PROGRAM OF  
RESEARCH ON HIGH TEMPERATURE MATERIALS  
Work Performed at the National Bureau of Standards  
Supported by the Advanced Research Projects Agency,  
Department of Defense

Edited by  
A. D. Franklin

1. INTRODUCTION

The National Bureau of Standards, with support from the Advanced Research Projects Agency of the Department of Defense, is carrying out a program of research on High Temperature Materials. In this program are included projects on their preparation, and others designed to explain the basic phenomena limiting the use of materials at high temperatures. A summary of the results achieved in the period is given here.

2. OBJECTIVES

One of the crucial factors limiting the advance of Defense technology is the failure of materials at elevated temperatures. This fact has long been recognized, and the Department of Defense has found it necessary to support a great deal of research to improve the high temperature performance of a wide variety of materials.

The continued success of these efforts depends upon having the right tools on hand when they are needed. In the case of advanced R&D, the tools include the science and practice of materials preparation and characterization, and of the measurement of materials properties. It is the overall objective of the present program to identify some of the more important of such key problems and to provide the needed advances where NBS possesses the competence to do so. These efforts will be directed mainly toward providing

techniques for the preparation and characterization of research materials, providing techniques for the measurement of properties, obtaining reliable values of key pieces of data, and improving the understanding of material properties particularly relevant to high-temperature performance.

In pursuit of this program, a continuing attempt is being made to analyze technological problems in high-temperature materials use and to distill from this analysis major scientific problems whose solution would advance the technology. In addition, the problems chosen should fall within areas in which NBS has front-rank competence available. As a final criterion, the number of problems included in the program should be small enough so that each one can be approached in a comprehensive fashion, ensuring adequate attention to specimen preparation and characterization.

In line with these criteria, the program is continuing to evolve. A further concentration of the work on fewer problems, perhaps one or two, will undoubtedly take place. One of these will be concerned with the diffusion of oxygen in oxides at high temperature. We are also examining the possibility of making an expanded study of the properties of transition metal borides as the focus of the rest of the program.

It is difficult to overemphasize the practical importance to DOD of improvements in the measurement of diffusion of metals and non-metals, particularly oxygen, in oxides. Diffusion is the process that controls the rate of attack on oxidation-resistant metals at high temperature, of corrosion (other than stress-corrosion) of many metals, of sintering of ceramics, swelling of reactor fuels, operation of ceramic fuel cells, and many other processes.

For instance, the corrosion and oxidation of structural metals at high temperatures is an outstanding problem

for DOD technology. The remedy lies in protection by some sort of coating, either deliberately applied or else formed during the early stages of corrosion. This coating must provide a barrier to the passage of ions, since for corrosion to proceed either oxygen must penetrate to the metal surface or metal ions must come out to meet the oxygen. The ultimate solutions to problems of this class will require understanding and control of the processes of diffusion in the oxide coatings.

At present the diffusion of ions in oxides is not at all well understood, nor subject to anything but very crude control. Among the major reasons are lack of sufficiently pure crystals upon which to make measurements; lack of reliable techniques for measuring diffusion rates, and therefore, of reliable diffusion data, particularly for oxygen diffusion; and lack of well-characterized grain-boundaries to assess the relative importance of bulk and grain-boundary diffusion in polycrystalline oxide ceramics and films.

Transition metal borides possess properties that promise considerable usefulness at very high temperatures. Thus, the diborides early in the transition metal series exhibit melting points in the neighborhood of 3000°C with the high thermal conductivities more characteristic of metals and with low thermal expansion. This combination of properties produces an excellent resistance to thermal shock. When combined with high chemical stability and oxidation resistance, they suggest promising materials where sudden extremes of temperature are encountered.

While considerable work has been done on a variety of borides, there is a very real need for the development of methods of preparing research-grade materials and for

characterizing them with respect to composition, purity, and homogeneity, and also with respect to lattice structure and perfection.

We are at present studying this problem area to determine if NBS can make a worthwhile contribution to the preparation of some of these borides at the research-grade level. If it appears that we can, it is planned to mount a research effort into the preparation techniques and such ancillary problems as high temperature and pressure phase equilibria. Specimens produced in this effort would form the basis for development of an electron-microprobe light-element-compound standard, and for continuation of our ongoing work (by J. R. Cuthill, et.al.) on the electronic structure of these materials. Studies on the chemical analysis of the borides, for major constituents and also for minor but important amounts of C, N, H, O, etc., would also be carried out. In the future, successful growth of good crystals would make possible work on lattice defects and their influence on mechanical properties.

### 3. PROJECT SUMMARIES

#### 3.1 Diffusion in Oxides

##### 3.1.1 Diffusion in Refractory Materials

A. L. Dragoo

Inorganic Materials Division

Institute for Materials Research

The objectives of this program are to measure and to interpret diffusion of oxygen in single crystal oxides. Experimentally these two objectives consist of (1) extending the sensitivity of present techniques so that the  $^{18}\text{O}$  distribution in a single crystal sample can be measured, (2) comparing the results of these concentration profile measurements with measurements of the rate of exchange of

$^{18}\text{O}$  between the gas phase and the oxide crystal, (3) determining the dependence of the diffusion rate on temperature, oxygen partial pressure, impurities in the solid, etc., and (4) obtaining reliable diffusion and exchange coefficients. In regard to interpretation, this objective translates into determining the mechanisms for oxide ion diffusion in the oxide studied. Currently, rutile ( $\text{TiO}_2$ ) is the oxide of interest. A mass spectrometer is being used to determine isotope ratios.

A major portion of the time during this period was spent in designing, and installing equipment. The isotope ratio mass spectrometer was finished by the Analytical Mass Spectrometry Section and moved into our laboratory. The installation of it is nearly completed. The graphite-reduction system for liberation of the oxygen from the oxide sample is undergoing modification to reduce the volume of the  $\text{CO-CO}_2$  conversion system and to improve the control of the conversion filaments. Construction of the manifold for the inlet system to the mass spectrometer is in progress.

In the previous report, mention was made of the solution of the diffusion equation for a problem involving competition between two different solid host media for the isotope in the vapor phase. Further details are given here, plus an approximate solution which was developed in order to have a convenient equation for the treatment of experimental data. This equation was applied to experimental data involving competition between an  $\text{Al}_2\text{O}_3$  furnace tube and a  $\text{TiO}_2$  sample for the  $^{18}\text{O}$  isotope in the vapor phase. We found that the experiment could be performed by nearly saturating the walls of the alumina tube before introducing the sample. The rate of depletion of  $^{18}\text{O}$  from the vapor phase was measured before and after introducing

the sample (a thin, single crystal, rutile wafer).

A mathematical description of the competition between two solid oxide diffusion media for  $^{18}\text{O}$  in the vapor phase was obtained by solving the diffusion equation,

$$\partial c / \partial t = D(\partial^2 c / \partial x^2)$$

for two models. The first model involved only one semi-infinite solid slab (called the tube) with a general continuous distribution of  $^{18}\text{O}$  whose surface was at all times in isotopic equilibrium with the vapor. The vapor was assumed to be finite and well stirred. The second model included a second semi-infinite solid slab (called the sample) along with the tube and vapor. The sample was assumed to have a normal uniform isotopic composition initially and its surface was assumed to be in equilibrium with the vapor at all times.

The two solutions were used to obtain a time-rate of change of  $^{18}\text{O}$  in the vapor phase. By subtracting the rate given by the first model from that given by the second model, a differential rate was obtained which contained both the independent effect of the sample and the interaction of the tube and sample.

Since the differential rate expression was very complicated, an approximation had to be found that was both convenient and accurate for the treatment of experimental data. A zero-order approach consisting of the elimination of all interaction terms agreed with simpler solutions of the diffusion equation. A first order expression was obtained by estimating the magnitude of each part of the interaction term of the differential rate expression. Since this term involved an integral containing an unspecified function which described the initial isotopic distribution in the wall of the tube, the contribution and form of this function

had to be considered. Noting that this function multiplied functions in the integrands which were nearly  $\delta$ -functions for short times and that it could be assumed to be equal to the initial mole fraction  $u_0$  of  $^{18}\text{O}$  in the gas (at  $t=0$ ), the integrations were easily performed by means of the property of the  $\delta$ -function

$$\int_{0-}^{\infty} f(\chi) \cdot \delta(\chi) d\chi = f(0) = u_0$$

The first approximation to the differential rate equation is

$$\frac{\partial u}{\partial t}_{1+2} - \frac{\partial u}{\partial t}_1 = (u_0 - v_{0,2}) \gamma \eta_2 \sqrt{D_2} [1/(\gamma \sqrt{\pi t}) + 1 - 2(1 + \gamma \sqrt{t}) \text{eerfc}(\gamma \sqrt{t})].$$

The various parameters are given in the accompanying table 1.

Table 1

$u_0$  = Initial mole fraction of the isotope in the gas

$v_{0,2}$  = Initial mole fraction of the isotope in the solid

$$\gamma = \eta_1 \sqrt{D_1} + \eta_2 \sqrt{D_2}$$

$\eta_i$  =  $A_i N_i / V_i N_g$ , where  $A_i$  is the area,  $V_i$  the volume,  $N_g$  the quantity of the diffusing element (all isotopes) in the gas and  $N_i$  the quantity of the element in the solid (the element is assumed to have the same molecular form in the solid phase as in the gas phase).

The subscripts 1 and 2 refer to the tube and sample, respectively. The special function  $\text{eerfc}(z)$  is defined by the equation

$$\text{eerfc}(z) = \exp(z^2) \cdot \text{erfc}(z)$$

where  $\text{erfc}(z)$  is the complimentary error function.

The above equation was used by Mr. F. P. Knudsen, of this laboratory, to treat data which he obtained for oxygen diffusion in rutile at 1350°C; he calculated

$$D = 2.19 \cdot 10^{-11} \text{ cm}^2/\text{s}$$

for the diffusion coefficient of rutile which can be compared with Haul and Dümbgen's [1] values

$$D = 1.73 \cdot 10^{-11} \text{ cm}^2/\text{s}, 1347^\circ\text{C}$$

$$D = 1.88 \cdot 10^{-11} \text{ cm}^2/\text{s}, 1348^\circ\text{C}.$$

In addition, he estimated that

$$D = 5 \cdot 10^{-12} \text{ cm}^2/\text{s}$$

for the tube.

#### References

- [1] Haul, R. and Dümbgen, G., J. Phys. Chem. Solids 26, pp. 1-10 (1965).

### 3.1.2 Diffusion of Oxygen in Oxides

F. P. Knudsen

Inorganic Materials Division

Institute for Materials Research

#### Introduction

This project is not an ARPA-sponsored project. However, the work is closely associated with, and virtually an integral part of, the research being done under the project



described in the preceding section, which is an ARPA sponsored project. For this reason, a report is submitted herewith to ARPA. Because of the integral nature of the two projects, this report will deal, in most instances, with combined efforts of both projects.

#### Objectives

(1) To obtain sound, reliable, data on the diffusion and exchange of oxygen in oxides, in such a manner that both the data and the experimental techniques will be widely accepted as standards and as a basis for comparison by experimenters using other unproven or controversial techniques.

(2) To improve the sensitivity and precision of the "sectioning method" of determining diffusion rates, so as to extend its applicability from the present diffusion coefficient limit of  $10^{-11}$  cm<sup>2</sup>/s to values as low as  $10^{-13}$  or  $10^{-14}$  cm<sup>2</sup>/s.

(3) To compare, by means of simultaneous experiments, the widely used, indirect, "gas depletion method" of determining diffusion rates with the direct "sectioning method" of determining diffusion rates.

(4) To define the pressure and temperature dependence of the diffusion of oxygen in oxides and to attempt to define the means by which oxygen diffusion occurs in the oxides under study.

#### Materials

Rutile (TiO<sub>2</sub>) was selected as the first oxide to be studied. Single crystal disks of rutile were obtained from a commercial supplier. The axis of each disk was parallel to the crystallographic c axis. The disks had been cut from boules specially grown by the supplier for this study. NBS spectrographic analysis of samples of

the disks showed .001 percent B as the only measureable trace element. Suspect traces of Al, Cu and Si were also noted.

Oxygen containing five percent of oxygen isotope 18 was used as tracer gas in the study. The isotope was obtained from a commercial supplier in the form of  $^{18}\text{O}$ -enriched water.

#### Summary of Previous Work

A rutile single crystal specimen was annealed for three weeks at 1350°C in normal research grade oxygen at a pressure of 1/3 atm in a platinum diffusion chamber to bring it into equilibrium with the anneal atmosphere with respect to oxygen activity, the latter being both temperature and pressure dependent. During this annealing treatment, platinum crystallites formed on the specimen. The crystallites caused small local irregularities in the contour of the specimen surfaces. These were removed by repolishing the faces of the specimen.

At this point, a consultant to the project expressed the opinion that the large thermal gradient in the diffusion chamber might cause some slight isotopic fractionation of any oxygen in the chamber. Gas samples taken during subsequent trial heatings disclosed that no measureable fractionation occurred under the test conditions.

However, during one of the trial heatings, a leak developed in the protective gas-tight alumina tube enclosing the platinum diffusion chamber. The platinum chamber was exposed to a compressive pressure differential of 2/3 atm at 1350°C. Although 0.15 mm thick, the chamber wall collapsed and sintered to itself, thereby ruining the chamber.

To continue the work while these difficulties (i.e. the deposition of platinum crystallites and the likely failure of another protective alumina tube) were being studied and overcome, the platinum chamber was temporarily replaced with one made of high-purity polycrystalline alumina. It was ascertained, by means of trial heatings and spectrographic analysis, that no measureable amount of alumina is adsorbed by rutile under the aforementioned experimental conditions. The attempt to use a polycrystalline alumina closed-end tube as a diffusion chamber met repeatedly with difficulty. Three such tubes, helium-gas-tight at room temperature, developed minute leaks at small flaws during use at 1350°C. To minimize the extraneous effect of the alumina chamber exchanging  $^{16}\text{O}$  for the  $^{18}\text{O}$ -enriched oxygen during diffusion anneals, the alumina tubes were pre-annealed for 3 weeks at 1500°C in the  $^{18}\text{O}$ -enriched oxygen at a pressure of 3/4 atm. From the depletion of  $^{18}\text{O}$  from the enriched oxygen during the satisfactory pre-anneal of the fourth alumina tube at 1500°C, a diffusion coefficient of  $2 \times 10^{-11} \text{ cm}^2/\text{s}$  was calculated for the diffusion of oxygen in this commercial alumina body having a nominal density of  $3.78 \text{ g/cm}^3$  and a nominal purity of +99.7%. The relative  $^{18}\text{O}$  content of samples of the enriched oxygen was determined by isotopic ratio mass spectrographic analysis at the University of Iowa.

Thereafter, the equilibrated rutile specimen mentioned earlier was diffusion-annealed in this fourth alumina chamber at 1350°C at 1/3 atm pressure of the  $^{18}\text{O}$  enriched oxygen tracer gas. The depletion of  $^{18}\text{O}$  from the enriched oxygen by diffusion into the crystal had to be distinguished from the associated extraneous depletion of  $^{18}\text{O}$  by diffusion into the polycrystalline alumina diffusion

chamber. With this objective, the enriched oxygen initially was permitted to diffuse into the alumina in the absence of the rutile crystal and thereafter the crystal was periodically introduced into and withdrawn from the high temperature diffusion region of the alumina chamber. Contrary to prior expectations, the precision of the experimental procedures and measurements proved to be sufficient to distinguish satisfactorily between the two rates of depletion of  $^{18}\text{O}$  from the tracer gas. However, the two simultaneous diffusion processes cannot be completely differentiated even by this means because they are not simply additive but interact with one another. In fact, slight evidence of the existence of this interaction was noted in the data of the periodic changes in the rate of depletion of  $^{18}\text{O}$  from the tracer gas. If the degree of interaction is assumed to be negligible, one obtains from the data of the above measurements, a value of  $(1.11 \pm .17) \times 10^{-11} \text{cm}^2/\text{s}$  for the coefficient of diffusion of oxygen parallel to the c axis in single crystal rutile at  $1350^\circ\text{C}$  in oxygen at a pressure of  $1/3$  atm. In order to provide a means of evaluating the degree of interaction and the diffusion coefficient in a manner which would properly compensate for the interaction, A. Dragoo derived a general equation for the competitive coupled diffusion process. The equation relates both diffusion coefficients of the coupled system to the time dependence of the difference between the observed two alternating rates of depletion of ambient tracer gas during a cyclic diffusion anneal, such as the one previously described. The diffusion coefficients can be evaluated by means of an approximation to the general equation. The general equation, its boundary conditions, the approximation, and the inherent assumptions therein,

are presented in the appendix to this section.

At the outset of the study, the projects had access to and part-time use of an isotope ratio mass spectrometer at the nearby University of Maryland. Although this arrangement was often inconvenient, analytical results could be obtained within twenty-four hours. Subsequently, the instrument was transferred to the University of Iowa where the analysis of samples was continued by the University on a fee basis. However, the three to six weeks usually required for the receipt of analytical results by this arrangement, forced the projects, in effect, to conduct their experiments blindly without any means of discovering the numerous possible daily errors or failures in established experimental procedures. Furthermore, as is obvious, it made the development of essential new experimental procedures and techniques unacceptably lengthy. A survey of nearby research facilities disclosed that there was no available isotope ratio mass spectrometer in this area. The need for such an instrument was clearly evident. In as much as the National Bureau of Standards had the skill, knowledge, facilities and experience to build such an instrument and could do so at a cost much less than that of a comparable commercial instrument, arrangements were made to have such an instrument constructed here at the National Bureau of Standards.

#### Progress in the Present Report Period

By means of the aforementioned diffusion equation approximation, the previously reported coefficient of  $1.11 \pm .17 \times 10^{-11} \text{ cm}^2/\text{s}$  for the self-diffusion of oxygen in rutile at  $1350^\circ\text{C}$  was recalculated without the use of the questionable presumption of the degree of interaction being negligible. The approximation and the evaluation of the

coefficient are presented in the appendix to the present report. When the interaction was taken properly into account, by the above means, a value of  $2.19 \times 10^{-11} \text{ cm}^2/\text{s}$  was obtained. For a comparable determination, other investigators, Haul and Dümbsgen [1] have reported a value of  $1.88 \times 10^{-11} \text{ cm}^2/\text{s}$ . Note, the degree of interaction was far from negligible, even though the chamber had been pre-saturated so thoroughly with the enriched oxygen that the relative  $^{18}\text{O}$  content of the ambient enriched oxygen decreased by only three percent during the diffusion anneal. Even of that slight decrease, only half was attributable to diffusion of the enriched oxygen into the chamber wall: Yet the interaction approximately doubled the value of the diffusion coefficient. This observation should prove to be of particular concern to other investigators using chambers capable of adsorbing or exchanging tracer gas.

Incidentally, the evaluation also yielded a value of  $5 \times 10^{-12} \text{ cm}^2/\text{s}$  as the diffusion coefficient of oxygen in the polycrystalline chamber wall at  $1350^\circ\text{C}$  in oxygen at a pressure of  $1/3 \text{ atm}$ . The determined values for the diffusion of oxygen in polycrystalline alumina,  $2 \times 10^{-11} \text{ cm}^2/\text{s}$  at  $1500^\circ\text{C}$  and  $5 \times 10^{-12} \text{ cm}^2/\text{s}$  at  $1350^\circ\text{C}$  are several orders of magnitude greater than the values reported by Oishi and Kingery [2] for polycrystalline alumina. The difference might be attributable to the fact that the nominal impurity content of the polycrystalline alumina tube chamber was approximately an order of magnitude greater than the impurity content of Oishi and Kingery's specimens.

The uncertainties and the more than twofold loss in time and precision in dealing with a coupled system, together with the complexity and controversial nature of the method of calculating the diffusion rates in such a

system, make it very undesirable to continue to use polycrystalline alumina as a diffusion chamber. The use of such a chamber was intended to be a temporary expedient.

In the interim, means have been found which presumably will overcome the difficulties previously encountered in the use of platinum as a diffusion chamber. The deposition of platinum crystals will be eliminated, or reduced to a tolerable degree (1) by suspending the diffusion specimen by a fine (i.e., approximately 0.04 mm diameter) single crystal sapphire filament instead of by fine platinum and platinum-rhodium thermocouple wires and (2) by decreasing or eliminating the appreciable quantity of water vapor formerly present in the  $^{18}\text{O}$  enriched oxygen tracer gas. The possibility of an accidental collapse of the platinum chamber will be eliminated by maintaining the pressure outside the chamber always equal to that within the chamber by means of a differential aneroid manostat.

The differential manostat and a suitable platinum chamber diffusion furnace were designed and constructed during the present report period while the projects were awaiting the completion of the construction of the isotope ratio mass spectrometer. The diffusion furnace consists of a closed-end platinum tube within a protective gas-tight polycrystalline alumina closed-end tube which, in turn, is within a molybdenum wire wound alumina heater core. The platinum chamber is fashioned of 0.08 mm thick platinum. It is 3.5 cm in diameter and 43 cm in length. The furnace components are joined together by high vacuum "O" ring seal flanges in such a manner that different gases can be maintained in isolation and regulated in the different sections of the furnace; that is, (1) within the platinum chamber, (2) between the platinum tube and the protective encompassing alumina tube and (3) within the section

external to the protective alumina tube (i.e., the section containing the heater core and the insulation of the furnace). The differential aneroid manometer is essentially comprised of a pair of sensitive three inch diameter bellows actuated by pressure changes within the diffusion chamber proper. The bellows directly actuate gas-tight seals connecting vacuum and bleed lines to the system immediately outside the platinum chamber.

In the simultaneous associate study of diffusion by the "sectioning method", a change in method of recovering the oxygen from the crystal sections was undertaken. The proposed change created the need for an apparatus for drying, encapsulating, and storing, ground sample sections, all continuously under vacuum. Such an apparatus was designed and constructed during the present report period.

Construction and installation of the isotope ratio mass spectrometer was virtually completed during the present report period and work is currently in progress on reassembling the diffusion system (i.e., diffusion furnace, gas handling system, hydrolysis cell, gas storage flasks, etc.) about the spectrometer and connecting the system thereto.

#### Objectives for the Next Report Period

To complete the reassembly and calibration of the various components and to proceed with the determination of the rate of oxygen self-diffusion in rutile as functions of temperature and pressure of ambient oxygen by both the "gas depletion method" and the "sectioning method".

#### References

- [1] Haul, R. and Dümbgen, G., "Sauerstoff-Selbstdiffusion in Rutilkristallen," J. Phys. Chem. Solids: Vol. 26, pp. 1-10 (1964).
- [2] Oishi, Y. and Kingery, W. D., "Self-Diffusion of Oxygen in Single Crystal and Polycrystalline Aluminum Oxide," J. Chem. Phys.; Vol. 33, No. 2, pp. 480-86 (1960).



## Appendix

A mathematical description of the competition between two solid oxide diffusion media for  $^{18}\text{O}$  in the vapor phase was obtained by solving the diffusion equation,

$$\frac{\partial c}{\partial t} = D \frac{\partial^2 c}{\partial x^2}$$

for two models. The first model involved only one semi-infinite solid slab (called the tube) with a general continuous distribution of  $^{18}\text{O}$  whose surface was at all times in isotopic equilibrium with the vapor. The vapor was assumed to be finite and well stirred. The second model included a second semi-infinite solid slab (called the sample) along with the tube and vapor. The sample was assumed to have a normal uniform isotopic composition initially and its surface was assumed to be in equilibrium with the vapor at all times.

The two solutions were used to obtain a time-rate of change of  $^{18}\text{O}$  in the vapor phase. By subtracting the rate given by the first model from that given by the second model, a differential rate was obtained which contained both the independent effect of the sample and the interaction of the tube and sample.

Since the differential rate expression was very complicated, an approximation had to be found that was both convenient and accurate for the treatment of experimental data. A first order expression was obtained by estimating the magnitude of each part of the interaction term of the differential rate expression. Since this term involved an integral containing an unspecified function  $f(\xi)$  which described the initial isotopic distribution in the wall of the tube, the contribution and form of this function had to

$$\gamma \quad \equiv \quad \frac{n_1}{a_1} - \frac{n_2}{a_2}$$

$$\frac{n_1}{a_1} \quad \equiv \quad \frac{A_1 n_1 \sqrt{D_1}}{V_1 n_g}$$

$A_1$   $\equiv$  the surface area of the interior of that portion of the alumina diffusion chamber approximately at the test temperature ( $\text{cm}^2$ )

$n_1$   $\equiv$  the quantity of total oxygen, taken as  $\text{O}_2$ , within the walls per se of that portion of the alumina diffusion chamber approximately at the test temperature (mol)

$n_g$   $\equiv$  the quantity of total oxygen, taken as  $\text{O}_2$ , in the gas within the entire diffusion chamber (mol)

$D_1$   $\equiv$  the diffusion coefficient of oxygen in the alumina ( $\text{cm}^2/\text{s}$ )

$V_1$   $\equiv$  the volume of solid of that portion of the alumina diffusion chamber approximately at the test temperature ( $\text{cm}^3$ )

$$\frac{n_2}{a_2} \quad \equiv \quad \frac{A_2 n_2 \sqrt{D_2}}{V_2 n_g}$$

$A_2$   $\equiv$  the surface area of the crystal specimen ( $\text{cm}^2$ )

$n_2$   $\equiv$  the quantity of total oxygen, taken as  $\text{O}_2$ , in the crystal specimen (mol)

$D_2$   $\equiv$  the diffusion coefficient of the crystal specimen ( $\text{cm}^2/\text{s}$ )

be considered. Noting that

$$f(0) = u_0$$

and that the terms multiplied by  $f(\xi)$  in the integral were approximately  $\delta$  functions, the integral was replaced by

$$\int_0^{\infty} f(\xi) \cdot \delta(\xi) d\xi = f(0) = u_0$$

The result is the following first order approximation,

$$\left(\frac{\partial u}{\partial t}\right)_{t+c} - \left(\frac{\partial u}{\partial t}\right) =$$

$$\gamma \left(\frac{n_2}{a_2}\right) (u_0 - v_{o_2}) \left\{ \frac{1}{\gamma\sqrt{\pi t}} + 1 - \right.$$

$$\left. \left[ 2e^{\gamma^2 t} \operatorname{erfc}(\gamma\sqrt{t}) \right] - \left[ (2e^{\gamma^2 t})_{\gamma\sqrt{t}} \operatorname{erfc}(\gamma\sqrt{t}) \right] \right\}$$

wherein:

$\left(\frac{\partial u}{\partial t}\right)_{t+c} \equiv$  the rate of change in the mole fraction of  $^{18}\text{O}$  in the gas in the diffusion chamber when the crystal specimen is in the chamber.

$\left(\frac{\partial u}{\partial t}\right)_t \equiv$  the theoretical rate of change in the mole fraction of  $^{18}\text{O}$  in the gas in the diffusion chamber had the specimen not been introduced into the chamber: the theoretical rate is calculated by extrapolation of the rate change observed prior to the introduction of the specimen.

- $V_2$   $\equiv$  the volume of the crystal specimen ( $\text{cm}^3$ )  
 $\frac{1}{a_1}$   $\equiv$   $\sqrt{D_1}$   
 $\frac{1}{a_2}$   $\equiv$   $\sqrt{D_2}$   
 $u_0$   $\equiv$  the mole fraction of  $^{18}\text{O}$  in the gas in the diffusion chamber at the time the crystal specimen was introduced into the chamber  
 $v_{\text{O}_2}$   $\equiv$  the mole fraction of  $^{18}\text{O}$  in the crystal specimen at the time it was introduced into the diffusion chamber  
 $t$   $\equiv$  the period of time subsequent to the introduction of the crystal specimen into the diffusion chamber (seconds)  
 $e$   $\equiv$  the Napierian base  $e$   
 $\text{erfc}$   $\equiv$  error function compliment  
 $T$   $\equiv$  the test temperature ( $^{\circ}\text{C}$ )  
 $P_0$   $\equiv$  the pressure of the gas within the time the crystal specimen was introduced into the chamber (Torr)  
 $w$   $\equiv$  the mass of the crystal specimen

Data

$A_1$	$200 \text{ cm}^2$ (estimated value)
$n_1/V_1$	$.058417 \text{ mol/cm}^3$
$n_g$	$.013893 \text{ mol}$
$A_2$	$4.146 \text{ cm}^2$

$n_2$  .0084193 mol  
 $V_2$  .1637 cm<sup>3</sup>  
 $u_0$  .088762  
 $v_{O_2}$  .0040683  
 $T$  1350 °C  
 $p_0$  316.35 Torr  
 $w$  .6727 g

By evaluating some of the terms in the equation and simplifying, one obtains,

$$\left( \frac{\partial u}{\partial t} \right)_{t+c} - \left( \frac{\partial u}{\partial t} \right)_t = - 1.299756 \gamma \sqrt{D_2} \left[ \frac{1}{\gamma \sqrt{\pi t}} + 1 - (1 + \gamma \sqrt{t}) 2e^{\gamma^2 t} \operatorname{erfc}(\gamma \sqrt{t}) \right]$$

wherein,

$$\gamma = \eta_1 \sqrt{D_1} + 15.34646 \sqrt{D_2}$$

The quantities,

$$(\eta_1 \sqrt{D_1}) \quad \text{and} \quad D_2$$

were evaluated by successive "least squares" approximations calculated to reduce the sum of the squares of their coefficients of variation to a minimum, where

$$\text{coefficient of variation} \equiv \frac{\text{LHS} - \text{RHS}}{\text{LHS}}$$

and:

LHS  $\equiv$  the value of the left hand side of the equation

RHS  $\equiv$  the value of the right hand side of the equation

The coefficient of variation was used in preference to the

variance because the values of the left hand side of the equation ranged over more than two orders of magnitude and because it was deemed likely that deviations would be proportional to the magnitude of LHS rather than constant.

The calculation of the "least squares" approximations encompassed values of  $(\eta_1\sqrt{D_1})$  ranging from  $1 \times 10^{-2}$  through  $1 \times 10^{-6}$  and values of  $D_2$  ranging from  $1 \times 10^{-9}$  through  $1 \times 10^{-13}$ .

The calculated "least squares" approximations were,

$$\begin{aligned}(\eta_1\sqrt{D_1}) &= 1.87 \times 10^{-3} \\ D_2 &= 2.19 \times 10^{-11}\end{aligned}$$

Accordingly, on the basis of the initial 48 hours of diffusion of  $^{18}\text{O}$  into the rutile crystal, parallel to the c axis.....

$$D_{1350^\circ\text{C}} = 2.19 \times 10^{-11} \text{ cm}^2/\text{s}$$

### 3.1.3 Crystal Growth From Vapor

H. S. Parker and C. A. Harding

Inorganic Materials Division

Institute for Materials Research

The objectives of this program are, first, the growth of aluminum oxide mono- and bicrystals of sufficient physical perfection and chemical purity for use as research materials; second, the reduction of both cation and anion impurities in vapor grown aluminum oxide crystals to sufficiently low levels to permit meaningful property measurements at the intrinsic level; and third, the extension of the technique to other materials of interest.

The major portion of the effort during this reporting

period has been devoted to the growth of bicrystals containing symmetrical tilt boundaries of a size and quality suitable for use as research specimens. Bicrystals of  $15^\circ$  and  $30^\circ$  misorientation have been grown, with either  $[11\bar{2}0]$  or  $[10\bar{1}0]$  as the rotation axis. In addition, vapor grown, self-seeded whiskers are being enlarged to a size sufficient for use as vapor grown seeds for subsequent bicrystal growth. Research-sized specimens of both mono- and bicrystals have been supplied to Drs. Heuer and Cooper at Case Western Reserve University for use in the ARPA program on Mass Transport in Oxides.

Various minor modifications to the growth equipment have been made with the intention of eliminating or minimizing possible sources of crystal contamination. As reported previously, activation analysis has indicated the chlorine content of the vapor grown crystals to be of the order of 70 parts per million or less. Spectrochemical analysis of crystals grown using ruby seeds and sapphire seeds shows that cation impurities are at quite low levels, as shown in the table.

#### Spectrochemical Analysis of $Al_2O_3$ Crystals

<u>Material</u>	<u>Impurities Found, % by Weight</u>
Ruby Seed Plate	Cu, Mg, Mn, Si - less than 0.001 Fe - questionable
Vapor Grown Crystal sapphire seeded	Cu, Mg, Mn, Si - less than 0.001 Fe - questionable
Vapor Grown Crystal, ruby seeded	Cu, Mg, Mn, Si - less than 0.001 Fe - questionable

The level of these impurities is at the lower limits of detection for the general qualitative spectrochemical technique utilized. Because of this, it is impossible to state whether any real differences exist among the samples

and seed. Discussions with personnel of the Analytical Chemistry Division of NBS indicate that by the use of a more sophisticated, semi-quantitative technique it may be possible to make definitive analyses at the 1-2 ppm level for copper and magnesium and at the 25 ppm level for silicon. The possibility of activation analysis for these impurities at these levels is currently under consideration.

A paper entitled "Vapor Growth of  $Al_2O_3$  Bicrystals" will be presented at the forthcoming ACCG-NBS Conference on Crystal Growth and subsequently submitted for publication.

Plans for the next period include an increased effort on both anion and cation impurity reduction in addition to supplying specimens for physical property measurements by other investigators.

### 3.2 Properties of Refractory Borides

#### 3.2.1 Electronic Structure of Refractory Hard Metals

J. R. Cuthill, L. H. Bennett, G. C. Carter

A. J. McAlister and I. D. Weisman

Metallurgy Division  
Institute for Materials Research

The objective of this project is to study changes in the density of states upon compound formation, especially in high temperature borides. The information should contribute to the understanding of the basic principles leading to the design of high temperature alloys with prescribed properties. The class of compounds being considered in this study are those binary and pseudo-binary compounds characterized by one of the constituents having an incomplete d or f shell and the other constituent having no d or f electrons. The transition metal borides, aluminides, and beryllides are examples.



Information is being obtained in the present study from soft x-ray spectroscopy, nuclear magnetic resonance, Mössbauer spectroscopy, magnetic susceptibility, and other probes of the electronic density of states.

The efforts during this report period could be divided into three categories: (1) Preparation and Characterization of Transition Metal Borides, (2) Physical Property Measurements of Transition Metal Borides, (3) Obscure Instrumental Corrections Peculiar to Investigations Involving Boron.

#### 1. Preparation and Characterization of Transition Metal Borides

Initial screening has indicated that specimens of  $\text{CrB}_2$ ,  $\text{VB}_2$  and  $\text{TiB}_2$  which we have in rod form and the following compounds which we have in powder form are more or less satisfactory for the measurements being made:  $\text{Fe}_2\text{B}$ ,  $\text{ScB}_2$ ,  $\text{TiB}_2$ ,  $\text{VB}_2$ ,  $\text{CrB}_2$ ,  $\text{VB}$ ,  $\text{CrB}$ ,  $\text{NiB}$ . The nuclear magnetic resonance spectra proved to be particularly useful as a characterization tool, quite apart from its value in revealing information on the electron density of states of these materials. One such instance was the mixed boride,  $\text{VCrB}_4$  having the  $\text{CrB}_2$  structure but with vanadium atoms substituting for Cr atoms on half of the chromium sites. The particular sample appeared from the x-ray diffraction pattern and from the metallography to be such a single phase structure. It was revealed by the NMR spectra (fig. 1) and independently confirmed by quantitative x-ray microanalysis that this particular specimen was in actuality merely a mixture of  $\text{VB}_2$  and  $\text{CrB}_2$  particles sintered but with little diffusion having taken place.

The  $\text{B}^{11}$  nuclear magnetic resonance spectrum from this specimen is shown in figure 1. The 2 pairs of peaks labelled "a" and "b" correspond to the quadrupole coupling

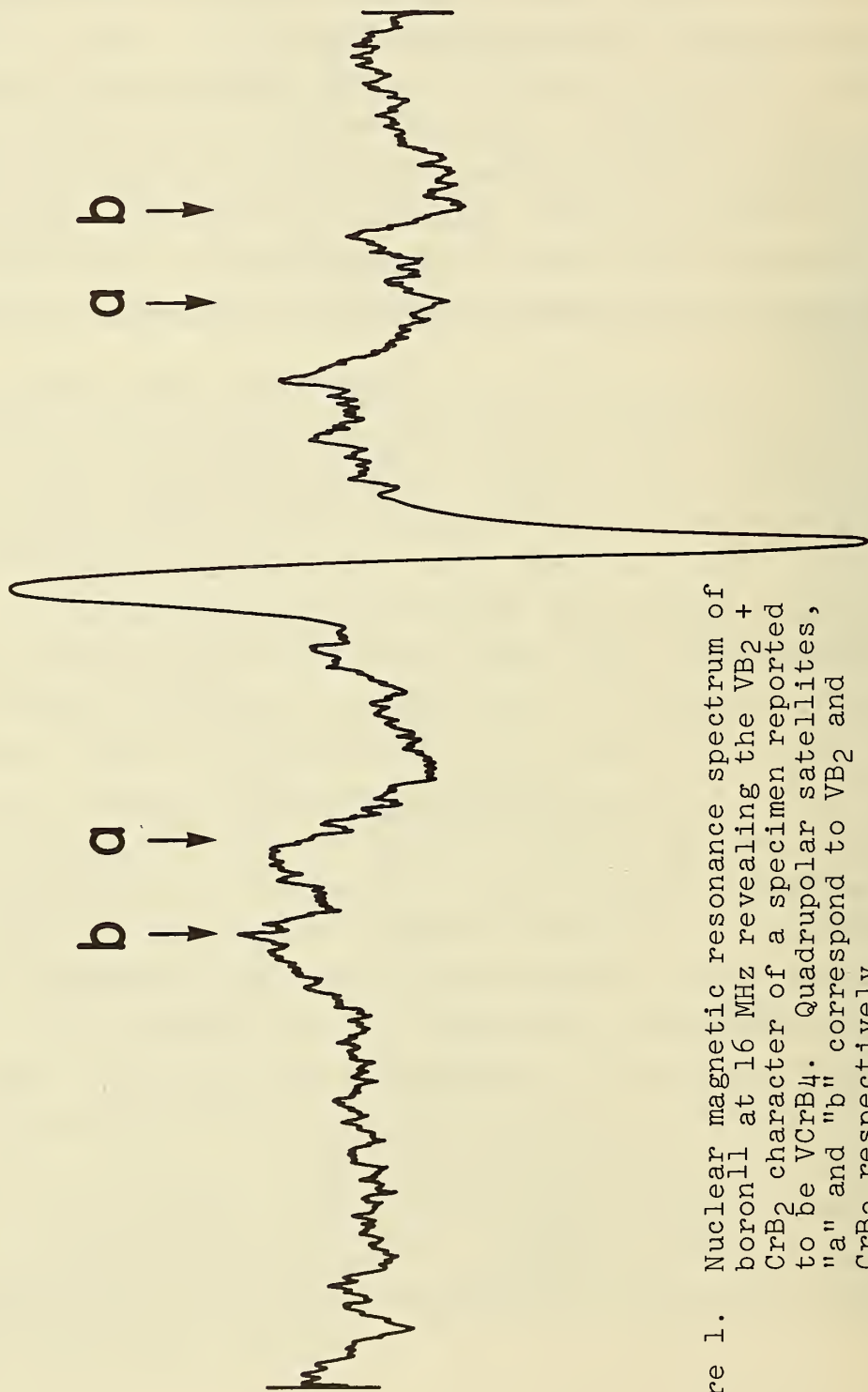


Figure 1. Nuclear magnetic resonance spectrum of boron-11 at 16 MHz revealing the  $\text{VB}_2 + \text{CrB}_2$  character of a specimen reported to be  $\text{VCrB}_4$ . Quadrupolar satellites, "a" and "b" correspond to  $\text{VB}_2$  and  $\text{CrB}_2$  respectively.

constants in  $\text{VB}_2$  and  $\text{CrB}_2$  respectively. The main boron resonance peak is at the same location and of the same width as it is in  $\text{CrB}_2$ . Only one  $\text{B}^{11}$  resonance is seen because the  $\text{B}^{11}$  resonance in  $\text{VB}_2$  is at the same location and is much weaker, so it is masked. The  $\text{V}^{51}$  resonance in this sample showed values for quadrupole constant and Knight shift that coincide with those of pure  $\text{VB}_2$ .

In the case of a specimen that was supposedly  $\text{NbB}_2$  the  $\text{B}^{11}$  resonance was typical of a single boride phase. The  $\text{Nb}^{93}$  resonance showed one resonance at the position of Nb metal and another one shifted from this to higher field (smaller Knight shift). This again indicated the presence of two phases, probably Nb metal and one of the niobium borides. In addition a hydrogen resonance was seen in this sample.

A last case in point here is our  $\text{MnB}_2$  sample of which the  $\text{B}^{11}$  resonance shows unexpected and unexplained oscillations when the field is swept. These oscillations have been found to be independent of the spectrometer frequency. Although this might be a true property of  $\text{MnB}_2$ , comparison with the results in other diborides suggest this experiment must be redone with a sample prepared with more certainty to be  $\text{MnB}_2$ .

These results clearly indicate the importance of specimen characterization by a variety of independent techniques. The literature contains a large body of physical as well as mechanical property data obtained from observations on specimens which have been inadequately characterized. As we have shown above, characterization by only one or even two techniques, such as x-ray diffraction and metallography is not sufficient, and published properties stemming from such investigations are open to considerable doubt.

## 2. Physical Property Measurements

Knight shift and quadrupole coupling constant measurements have been continued. In the diborides our values are in substantial agreement with values found in the literature, where such data are available. The diborides studied include  $\text{ScB}_2$ ,  $\text{TiB}_2$ ,  $\text{VB}_2$ ,  $\text{CrB}_2$ ,  $\text{MnB}_2$ ,  $\text{NbB}_2$ . The boron resonances shown a central line with a Knight shift between  $-0.01$  and  $-0.05\%$  with respect to triethyl borate. The  $\text{V}^{51}$  resonance shows a negative Knight-shift with a negligible temperature dependence down to  $77^\circ\text{K}$ . The  $\text{Sc}^{45}$  resonance in  $\text{ScB}_2$ , observed for the first time, shows strong second order quadrupole effects, having a quadrupole coupling constant of near  $6.2$  MHz.

Preliminary measurements on transition metal monoborides have been undertaken by NMR. An extensive literature search revealed no previous work on monoborides. Samples we have studied include  $\text{NiB}$ ,  $\text{VB}$ ,  $\text{CrB}$ ,  $\text{NbB}$ , with shifts ranging from  $-0.04$  to  $-0.16\%$ . The resonance lines show additional structure in the wings which in a few cases can be interpreted as quadrupole satellites. Two other samples studied are  $\text{Cr}_2\text{B}$  and  $\text{Cr}_5\text{B}_3$ .

## 3. Obscure Instrumental Corrections Peculiar to Investigations Involving Boron

Boron, or boron compounds occur in various components normally used in laboratory equipment and produces signals which must either be removed or corrected for. Often the boron signal due to the apparatus is not suspected and causes complications and uncertainties in data reduction.

In the course of our work we have seen structure in the central resonance which was determined to be the signal of the boron in the NMR probe. This was done by directly integrating the signal of the probe and sample in the add

mode of an on-line computer and subtracting out an equivalent number of scans of the probe signal with the sample removed. The  $B^{11}$  resonance in VB gave the most clear example of this interference. Others also report similar spurious central structure in some diborides but failed to account for its origin.

Another source of spurious boron signal in the NMR spectra was found to be the boron in the glass dewars being used. Also, boron was detected in soft x-ray spectra of materials which should not have contained boron. A boron nitride insulator which was not in the electron beam but was heated moderately by the thermal radiation was found to be responsible for the boron emission.

#### Papers Published During This Report Period

1. Resonance Studies in Ferromagnetic  $Fe_2B$  and  $Fe_2Zr$ , I. W. Weisman, L. J. Swartzendruber, and L. H. Bennett, Phys. Rev., 177, 465-471, 10 January 1969.
2. Magnetic Behavior of Intermetallic Compounds of Beryllium, N. M. Wolcott, R. L. Falge, Jr., and L. H. Bennett, J. Appl. Phys. 40, 1377-1378, 1 March 1969.

### 3.3 HIGH TEMPERATURE METALS

#### 3.3.1 Optical Constants of Titanium in The Visible Region of Spectrum

A. J. Melmed

Metallurgy Division

Institute for Materials Research

Efforts during the period of this report were directed

- 1) towards building an ultrahigh vacuum system and a tube for making optical constants measurements on titanium characterized in situ as clean by low-energy-electron diffraction

techniques, and 2) towards establishing techniques for meaningful measurements of optical constants using vapor-deposited titanium films.

The ultrahigh vacuum system has been assembled and is being tested. The experimental tube is about 90% completed. Special care was taken in its design and construction to ensure that the fused-quartz windows for entry and exit of polarized light were strain-free and accurately aligned for proper ellipsometric measurements. These important considerations are frequently neglected and can cause serious errors in optical constants measurements, especially in vacuum. The windows in the new tube were designed so that they could be completely oven-annealed and were tested with our ellipsometer. No evidence of strain was detected.

We began a series of experiments with evaporated metal films. Before working with titanium films we tried iron films, since reliable modern measurements have been reported for the optical constants of bulk iron cleaned and measured in ultrahigh vacuum. Thus a good basis for comparison of results was available. This was felt necessary in order to establish that measurements made on evaporated films gave optical constants for the bulk metal. We found that iron films vapor-deposited on a previously cleaned single-crystal (011)-oriented tungsten substrate exhibited optical constants (in the visible spectral range) which changed with film thickness and reached limiting values in good agreement ( $\sim 1\%$ ) with the most recently published bulk iron optical constants provided the films were briefly ( $\sim 10$  sec.) annealed. The thickness necessary for this agreement was about 300-400Å, determined by ellipsometry. The film formation process was also followed by LEED on the same specimen and by tungsten field-electron emitter located approximately at

the same distance from the metal vapor source. These techniques showed that the as-deposited film was very granular with grain sizes of the order of  $\sim 200\text{\AA}$ , and had very little long-range order. After annealing (temperature  $< 600^\circ\text{C}$ ) long-range crystallographic order was apparent and the film was epitaxially oriented, with the (011) planes parallel to the (011) planes of the substrate and with a measured lattice constant agreeing within  $\sim 1\%$  with the accepted value.

We have therefore begun experiments of a similar type with titanium. To date, the ellipsometry data looks normal, but there appears to be a complication in interpreting the LEED results. We are presently analyzing the data.

### 3.3.2 High Temperature Creep in Metals

A. A. O. Rukwied, W. A. Willard, D. E. Harne  
Metallurgy Division

Institute for Materials Research

The objectives of this investigation are to investigate the microscopic mechanisms that control high temperature creep, i.e., creep occurring at temperature  $T > T_m/2$ , where  $T_m$  is the melting point. More specifically it is planned to study: (a) the effect of temperature on the creep rate and compare this to the temperature dependence of dislocation velocity, (b) the effect of stress and compare this to measurement of dislocation density carried out by etch pit techniques, (c) study the effect of stacking fault energy through its variation in an alloy series and (d) study the effect of grain boundaries by comparison of studies in single crystals and polycrystals. For these studies copper and copper-alloys have been selected to begin with especially since etch pit techniques for these materials are already developed.

The work on polycrystalline high purity copper which was the subject of previous progress reports has been

continued by obtaining and measuring high temperature creep curves as a function of temperature at two more stress levels. All the creep data obtained so far have been evaluated and analyzed. They will be presented here in a preliminary form.

The apparent activation energies derived from measurements of the second stage creep rates turned out to be practically constant over the whole range of temperature covered, and with the values  $U_c = (176 \pm 6.3) \text{ kJ/mol}$ , or  $(42 \pm 1.5) \text{ kcal/mol}$ , were about 10 to 20% smaller than the activation energy for self diffusion which may be assumed to be somewhere between  $197 \text{ kJ/mol}$ , or  $47.1 \text{ kcal/mol}$ , (Kuper et. al. Phys. Rev., 96 (1954), p. 1224) and the latest measurement of  $211 \text{ J/mol}$ , or  $50.5 \text{ kcal/mol}$  (Rothman et. al., APS Meeting, Chicago, March 1969).

This finding differs in two major points from the measurements reported by Barrett and Sherby in the literature:

(1) Within a temperature interval of  $260^\circ\text{C}$  the apparent activation energy for high temperature creep was found to be constant, demonstrating that one single rate controlling mechanism operates over the entire temperature interval. This interval includes the temperature of transition of the apparent activation energy from a lower value ( $117 \text{ kJ/mol}$ , or  $28 \text{ kcal/mol}$ ) to the one for self diffusion ( $201 \text{ kJ/mol}$ , or  $48 \text{ kcal/mol}$ ), as reported by Barrett and Sherby.

(2) The value of the apparent activation energy agrees neither with the lower, nor with the higher, value given by Barrett and Sherby, but is closer to the higher value, the one for self diffusion.

An explanation for this discrepancy necessitates a check of various factors, such as purity, test procedures, etc., which might affect creep properties. A comparison of some of these factors is given in table 1.



Table 1. Comparison of Factors Affecting Creep

	Barrett and Sherby	Present Work
(1) Material	OFHC Copper, purity better than 99.995% (8 ppm Ag, 2 ppm Ca, 2 ppm H <sub>2</sub> , 20 ppm O <sub>2</sub> )	ASARCO Hi-Purity Copper nominal 99.999% purity (analyzed to contain: 2 ppm O <sub>2</sub> , 2 ppm N <sub>2</sub> , no H <sub>2</sub> , 3.5 ppm C, 0.1 ppm Al, 0.1 ppm Mg, 0.1 ppm Si. Material containing a cellular solidification substructure.
(2) Specimen-preparation	Polished with 2/0 emery paper before annealing	No abrasives
(3) Atmosphere	Dry deoxidized H <sub>2</sub> , or vacuum	Purified He
(4) Loading	Constant stress	Constant load
(5) Grain sizes	0.03 (3000 psi), 0.4 (3000 psi) and 1.0 mm (at 500 and 1500 psi)	1.0 mm all stresses
(6) Annealing treatment and grain size	700°C/5 min: 0.03 mm grain size 800°C/30 min: 0.4 mm grain size 1000°C/60 min: 1.0 mm grain size	800°C/16 hrs: 1.0 mm grain size
(7) U <sub>c</sub> -determination	Cycling and isothermal tests yielding agreement of values	Isothermal tests only

If we discount the constant load type test as being responsible for the observed discrepancy\*, we have to attribute responsibility to structural factors in our material other than grain size and dislocation density. Therefore an extensive study was undertaken using optical and electron microscopy correlated with etch pit experiments, to better characterize the test material. As a result, a cellular solidification substructure was found, due to segregation of impurities during continuous casting in a constitutionally supercooled melt.

On an electropolished and etched surface, the region of the crystal to which segregation has occurred is distinguished by clusters and rows of etch pits, the result of a preferred attack by the etchant. Within this region cells of densely tangled dislocations have been observed. After cold work, recrystallization and prolonged annealing treatment at relatively high temperature (800°C/20 hrs), the solidification substructure can still be revealed by etch pitting. However, small particles in the segregated region could not be revealed unambiguously, although at least solid solubility measurements of carbon in copper strongly suggest the formation of carbon particles during solidification. Since carbon can be in solid solution in equilibrium at the melting point of copper at a concentration of 7 ppm only, and the overall carbon concentration in our material is 3.5 ppm, precipitation of carbon must

---

\* One can make an estimate on the effect of testing under constant load as compared with constant stress. Using the relation  $\epsilon \propto \sigma^{4.8}$  it can be shown, that constant load tests measure activation energies not more than 6.3 kJ/mol, or 1.5 kcal/mol, greater than constant stress tests.

occur due to the rise of carbon concentration in the region in which segregation does occur. Similar considerations should hold for the other possible contaminants in the test material, like oxides of Cu, Al, Mg, Si and silicon carbide which are present in trace concentrations. Thus, since bigger particles are not observed, their size must be smaller than 5 to 8 nm (50 to 80Å) and the particles are probably finely dispersed in the solidification substructure. The thermal stability and low mobility of the solidification substructure up to the melting point of copper explain the mechanical and thermal stability of the solidification substructure.

In summary we can state the following points which are relative to the copper used for the creep tests:

(1) After the annealing treatment the main fraction of the impurities are still in the substructure arising from cellular solidification.

(2) The impurities contained in the test material have very low or no mobility at the creep test temperatures.

(3) We have to expect the existence of small second phase particles in the growth substructure, but since they could not be seen directly, the particle size probably is less than 5 to 8 nm, or 50 to 80Å.

(4) The regions of the crystal bounded by the segregation substructure probably has a high degree of purity and perfection.

(5) The dislocation density is low.

(6) So far - and this is to be taken as a very preliminary statement - no interaction has been observed to have taken place between the remainders of the cellular solidification structure and the dislocation cells formed during creep.

Returning to the observed apparent activation energy for second stage creep, Barrett and Sherby argue that the lower apparent activation energy level in copper is due to dislocation-enhanced diffusion of vacancies. Following Hart (Acta Met., 5 (1957), p. 597) they represent the macroscopically observed effective self diffusion coefficient as a volume weighted sum of dislocation and lattice diffusivity

$$D_{\text{eff}} = D_d (g) + D_e (1-g),$$

$D_d$  - dislocation diffusivity  
 $D_e$  - lattice diffusivity  
 $g$  - lattice site fraction in  
           high diffusivity region  
           around dislocations

indicating that, depending upon the temperature,  $D_d$ ,  $D_e$ , or both can determine the effective diffusion coefficient, and should therefore manifest themselves in the temperature dependence of the apparent activation energy for high temperature creep.

If we want to explain the value of the apparent activation energy measured by us in such a model of enhanced diffusivity, we have to find a diffusion path that is easier than self diffusion, and faster than dislocation enhanced diffusion within the temperature range in question. We would like to suggest that such a diffusion path could be provided by the segregation substructure, which interconnects the entire material by a regularly spaced channel system, consisting of "columns" and walls distorted by a relatively high solute concentration, which might be of the order of 1%, and very probably by the presence of second phase particles of a size not resolvable by the electron microscope, in the segregation region. In such a model a transition to another rate controlling process of steady

state creep characterized by the self-diffusion activation energy may be expected at a higher temperature, and a transition to a lower apparent activation energy due to dislocation-enhanced diffusion at lower temperatures, cannot be excluded. The low dislocation density, since it enters the preexponential term of the diffusivity, could probably help to shift downwards the temperature of transition to creep controlled by dislocation-enhanced diffusion. As a consequence of the assumption that the diffusivity in the segregated region controls second stage creep, one should expect the rate controlling creep process to take place within the region containing the segregation substructure. We are working on that problem presently, but have not yet obtained conclusive evidence.

In conclusion it should be emphasized, that in high purity fcc materials a very careful characterization with respect to impurity content and distribution is imperative for high temperature creep tests. It is obvious that more tests varying these parameters are needed to clarify their roles in high temperature creep.

#### On the definitions of creep stages I and II:

Data being obtained in creep tests indicate that a redefinition may be in order for steady state or minimum creep rates. Consideration is being given to the best way to redefine these stages.

#### SUMMARY:

(1) High temperature creep tests have been carried out on high purity copper in a high purity He atmosphere. The test material contained a cellular solidification substructure.

(2) The starting material for the creep tests is being characterized using optical and electron microscopy.

(3) The apparent activation energy for steady state creep has been measured from isothermal tests in the temperature range between 440 and 702°C.  $U_c$  has been found to be constant over the entire temperature range and with a value of 176 kJ/mol, or 42 kcal/mol, to be about 10 to 20% smaller than the activation energy for self diffusion. This value is probably somewhat higher than a value one would derive from creep tests carried out at constant stress.

(4) It has been suggested that this value of  $U_c$  is due to lattice distortion-enhanced diffusion along the cellular solidification substructure.

(5) Consideration is being given to a redefinition of creep stages I and II.

The constant resolved shear stress creep testing unit was finally accepted from SATEC Systems, Inc. No time however has been available since to take it into operation and to do research work, because the study on the copper polycrystals had to be brought to a point from which a publication of results obtained so far, is within reach.

### 3.4 CERAMICS

#### 3.4.1 Deformation and Fracture of Ionic Crystals

S. M. Wiederhorn and L. H. Bolz

Inorganic Materials Division

Institute for Materials Research

Research on this project has been directed towards understanding brittle failure of ceramic materials. Glass has been chosen as an object of study because of its commercial importance and because it serves as a model material for failure of other high temperature ceramic materials.

Stress corrosion cracking data has been obtained to elucidate the failure mechanisms in a variety of glasses.

In the last report it was stated that crack velocity data, obtained in liquid water as a function of temperature, satisfied the Charles-Hillig theory for stress corrosion. Experimental data has been found to fit an equation of the form  $v = v_0 \exp[-(E^* - bK_I)/RT]$ , where  $v$  is the velocity,  $v_0$  is a pre-exponential constant,  $E^*$  an activation energy,  $b$  a constant and  $K_I$  the stress intensity factor. During this period the data has been analyzed and it is believed that the rate limiting step in the corrosion reaction involves a direct attack of the hydroxyl radicals on the silicon oxygen network. This conclusion is based on the following experimental evidence:

1. The pre-exponential of the above equation is directly proportional to the  $[OH^-]$  of glasses ground up in limited amounts of water.
2. The activation energy, after a correction for the  $[OH^-]$  temperature dependence, is approximately 92 J/mol, or 22 kcal/mol for all glasses tested, and is close to that obtained for known  $OH^-$  attack on glass.

Some data is still being collected on the stress corrosion process. When finished a paper will be submitted for publication in the Journal of the American Ceramic Society.

#### Papers Published During This Report Period

1. S. M. Wiederhorn, "Fracture Surface Energy of Glass", J. Am. Ceramic Society, 52 (2) 99-105 (1969).
2. S. M. Wiederhorn, "Fracture of Ceramics" from Mechanical & Thermal Properties of Ceramics, Editor, J. B. Wachtman, Jr.; NBS Special Publication - 303, May 1969.

## 3.5 POLYMERS

### 3.5.1 The Volatilization and Decomposition of Materials

L. Wall and S. Straus

Polymers Division

Institute for Materials Research

The rates of vaporization of five aromatic compounds were measured as a function of temperature and their activation energies obtained. In terms of kinetic theory for vaporization the activation energy  $E_v$  for vaporization is related to the heat of vaporization at the temperature of the measurement, by the relation,

$$E_v = \Delta H_v - \frac{3}{2}RT$$

Table 1 now includes all the phenylene ether type compounds we have available for study. The fifth compound listed which was previously reported had not behaved like a pure compound.

This 7-unit meta linked phenylene ether compound, m-bis[m-(m-phenoxy phenoxy)phenoxy] benzene, was purified by collecting the middle fraction on distillation. This fraction, when heated in vacuum at 211, 220, 227, and 233°C, vaporized at a constant rate independent of the amount vaporized, indicating more clearly a volatilization of a pure compound. Previously the rate had decreased rather than remaining constant as vaporization proceeded. The activation energy, for the purified sample, was calculated to be 134 J/mol, or 32 kcal/mol, similar to the previous value for the extrapolated slopes.

The results in table 1 show that for the first 5 compounds, which are a series of meta-linked phenylene ethers, the energy increment per unit decreases above the 5 unit species with the larger compounds. This is evidence that



Table 1. Experimental Activation Energies for  
Molecular Vaporization

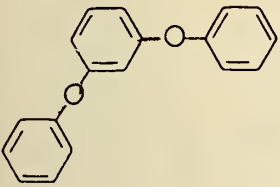
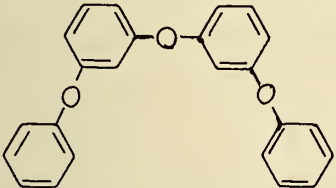
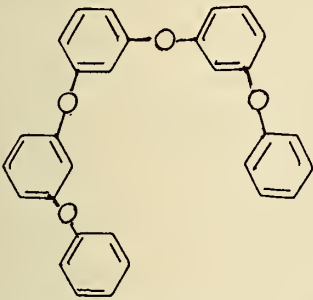
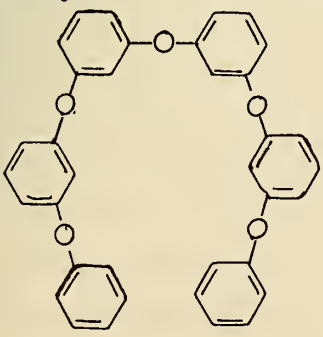
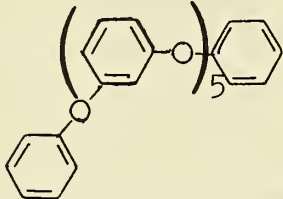
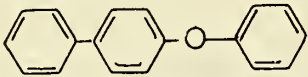
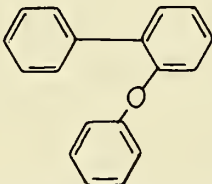
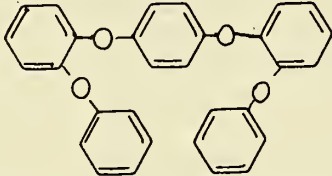
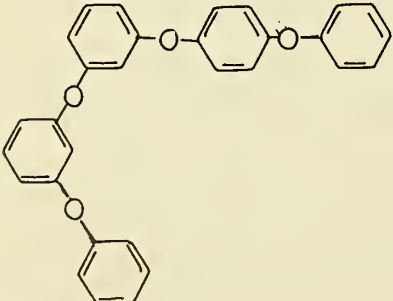
Compound	Formula	M.W.	$E_v$ kcal/mol
m-diphenoxy benzene 	$H(C_6H_4O)_2C_6H_5$	262.32	15
bis(m-phenoxy phenyl)ether 	$H(C_6H_4O)_3C_6H_5$	354.41	20
m-bis(m-phenoxy phenoxy) 	$H(C_6H_4O)_4C_6H_5$	446.00	25
bis[m(m-phenoxy phenoxy) phenyl]ether 	$H(C_6H_4O)_5C_6H_5$	538.60	29

Table 1. Continued

Compound	Formula	M.W.	$E_v$ kcal/mol
m-bis[m(m-phenoxy phenoxy) phenoxy]benzene	$H\langle C_6H_4O \rangle_6 C_6H_5$	630.70	32
			
4-phenyl phenyl ether (para)	$C_6H_5C_6H_4OC_6H_5$	246.31	23
			
2-phenyl phenyl ether (ortho)	$C_6H_5C_6H_4OC_6H_5$	246.31	16
			
p-bis(o-phenoxy phenoxy) benzene	$H\langle C_6H_4O \rangle_4 C_6H_5$	446.50	25
			
m-(m-phenoxy phenoxy) phenyl-p-phenoxy phenyl ether	$H\langle C_6H_4O \rangle_4 C_6H_5$	446.50	24
			

the larger species can evaporate with a dense conformation minimizing the energy requirement. Work is continuing with purification, preparation and activation energy measurements of various linear and non-linear ester structures.

### 3.5.2 Relaxations Near the Melting Point

J. P. Colson and R. K. Eby

Polymers Division

Institute for Materials Research

If the dynamic mechanical properties of mats of solution-grown crystals of polyethylene are measured with a torsion pendulum, the strength of the  $\alpha$  (higher temperature) relaxation depends upon the temperature at which the crystals have been annealed. Furthermore, the magnitude of the relaxation correlates with the reciprocal of the thickness of the crystals. This has been interpreted as meaning that the origin of the relaxation is in the crystal surface. However, we have previously shown that the area of the basal (a, b) plane of the unit cell also correlates with the strength of the  $\alpha$  relaxation. We have now found yet another correlation between the  $\alpha$  relaxation and one of the parameters necessary to describe completely the crystal mats. This parameter is the small residual solvent left in the mats from the preparation process. As the crystals are annealed at higher temperatures, the solvent content decreases in a fashion which corresponds with the decrease of the strength of the  $\alpha$  relaxation. We are not prepared at present to interpret the correlations of the solvent content and the cell dimensions with the strength of the  $\alpha$  relaxation. However, they do show that there is some question about the significance of the correlation with the reciprocal of the crystal thickness since this correlation is not unique. Clearly there is a need for more research to determine the mechanism which leads to these correlations.

## 3.6. LASER MATERIALS

### 3.6.1. BULK OPTICAL PROPERTIES OF LASER MATERIALS

G. W. Cleek and R. M. Waxler

Inorganic Materials Division

Institute for Materials Research

#### Objectives

This project was established with the objective of evaluating the bulk optical properties of laser crystals and glasses, particularly synthetic single crystal ruby and neodymium-doped glass. These data are needed to calculate the corrections for the distortion of the wave front in light generated by lasers. The distortion is produced by thermal effects when the rods are operated.

Specifically, determinations are being made of the appropriate thermo-optic and elasto-optic properties required for the above calculations, as well as other properties needed to characterize these materials.

#### Technical Approach

Measurements are being made on commercially available ruby and neodymium-doped glasses. The single crystal ruby was doped with 0.05% Cr. Five specimens of neodymium-doped glasses have been received. These are identified as samples A, B, C, D, and E. The properties that have been determined during this reporting period on each of the specimens are discussed below.

#### Property Measurements

##### Photoelastic Constants

##### (a) Ruby

Since the last semi-annual report, the two remaining piezo-optic constants,  $q_{14}$  and  $q_{44}$ , have been measured for single-crystal ruby. The entire set of eight  $q_{ij}$  has now been determined and the results are given in table 1. A check of calculations showed that some values given in the

Table 1. The photoelastic constants of synthetic ruby doped with 0.05% Cr.

piezo-optic constants

$q_{11}$	$q_{33}$	$q_{12}$	$q_{13}$	$q_{14}$	$q_{31}$	$q_{41}$	$q_{44}$
$\times 10^7 \text{ bar}^{-1}$							
-0.52	-.41	.08	.13	-.07	.01	-.01	-.71

elasto-optic constants

$p_{11}$	$p_{33}$	$p_{12}$	$p_{13}$	$p_{14}$	$p_{31}$	$p_{41}$	$p_{44}$
-0.23	-.20	-.03	.02	.00	-.04	.01	-.10

last semi-annual report were in error; the correct values are given in table 1.

Using the data of Wachtman [1] for values of the elastic moduli,  $c_{ij}$ , the eight elasto-optic constants,  $P_{ij}$ , have been evaluated according to the equation

$$P_{ij} = \sum_{k=1}^6 q_{ik} c_{kj} \quad (1)$$

and the results are also given in table 1.

The phenomenological theory of photoelasticity developed by F. Pockels [2,3] assumes that the elastic deformations and not the stresses are primarily responsible for the changes in refractive index. It is interesting to note that for ruby (table 1)  $p_{11}$ ,  $p_{33}$ ,  $p_{12}$  and  $p_{31}$  all show negative values. Of all the crystals topaz and diamond and the partly covalent crystal MgO, exhibit negative values for  $p_{hk}$  ( $h, k = 1, 2, 3$ ). In topaz it is found that  $p_{11}$ ,  $p_{22}$  and  $p_{33}$  are all negative in value. MgO has negative values for both  $p_{11}$  and  $p_{12}$ ,

while diamond has a negative value for  $p_{11}$  only. All these crystals are noted for having strong interatomic bonding.

Also, it may be seen in table 1 that  $p_{44}$  is of the same order of magnitude as the other constants. This is typical of covalent crystals where it is found that, in general,  $p_{\ell\ell}$  ( $\ell = 4,5,6$ ) are of the same order of magnitude as  $p_{hk}$  ( $h,k = 1,2,3$ ). This is not the case in ionic crystals where the  $p_{\ell\ell}$  are much smaller than the  $p_{hk}$  [3].

Mueller [4,3] has developed a physical theory to explain the changes in the refractive index ellipsoid that take place when a solid is stressed. In this theory, calculations are made of the changes in the density, the Coulomb field, the Lorentz-Lorenz field, and the intrinsic polarizability of the scattering centers. The contribution of density is always positive and in most crystals exceeds the combined effect of the other three changes so that the  $p_{hk}$  are generally positive. The theory has been worked out for glasses and cubic crystals, but not for crystals of lower symmetry such as ruby (crystal class  $\bar{3}m$ ) where the computations become extremely complicated. Although the individual contributions can not be calculated out for ruby, it may be noted that the combination of the latter three changes outweighs the contribution due to change in density and, with the exception of  $p_{13}$ , the  $p_{hk}$  of ruby have negative values. Even with  $p_{13}$ , the positive numerical value is very small ( $p_{13} = .01$ ).

The photoelastic constants of calcite have been determined by Pockels [5,3], and it is interesting to compare these data with the results on ruby because both crystals belong to class  $\bar{3}m$ . In both crystals the oxygen atoms are arranged in triangular groups perpendicular to the optic axis. However calcite has a true layer lattice, whereas

$Al_2O_3$  possesses an isosthenic lattice in which the oxygen atoms are almost in hexagonal close packing. The elastic compliances of calcite are much greater than those of ruby [3]. This pronounced difference in the elastic compliances manifests itself in the photoelastic constants where it is found that the  $p_{hk}$  of calcite are all positive, and the  $p_{hk}$  of ruby are generally negative.

(b) Neodymium-doped laser glasses

The two piezo-optic constants,  $q_{11}$  and  $q_{12}$ , and two elasto-optic constants,  $p_{11}$  and  $p_{12}$ , have been determined for the five neodymium-doped glasses, and the results are given in table 2. It can be seen in table 2 that the values

Table 2. The photoelastic constants of neodymium doped laser glasses

GLASS	$(q_{12}-q_{11}) \times 10^7$	$q_{11} \times 10^7$	$q_{12} \times 10^7$	$p_{11}$	$p_{12}$
	bar <sup>-1</sup>	bar <sup>-1</sup>	bar <sup>-1</sup>		
A	1.64	0.53	2.16	0.134	0.225
B	1.59	.58	2.18	.139	.222
C	1.58	.78	2.36	.153	.232
D	1.49	.54	2.04	.139	.218
E	1.09	.12	1.21	.105	.184

for the various glasses are largely the same, with the exception of the sample E glass where the values are markedly different. This difference may be attributed to the fact that the composition of the sample E glass differs notably from the other glasses as shown in table 3. It may be noted that the optical measurements on the samples B

Table 3. Major constituents in wt.% in Nd-doped glasses as determined by chemical analysis

Oxide	A	B*	C	D	E*
SiO <sub>2</sub>	66.56	>10	>10	60.31	>10
Al <sub>2</sub> O <sub>3</sub>	1.80	0.1-1	0.1-1	1.91	1-10
BaO	5.46	1-10	1-10	3.02	
K <sub>2</sub> O	10.06	1-10	1-10	17.14	
Na <sub>2</sub> O	6.56	1-10	1-10	5.88	
Li <sub>2</sub> O	1.03			.93	1-10
Sb <sub>2</sub> O <sub>3</sub>	0.73	0.1-1	1-10	0.73	
PbO		1-10	1-10		
ZnO	1.57			1.82	
Nd <sub>2</sub> O <sub>3</sub>	5.35	1-10	1-10	5.81	1-10
CaO		0.01-.1	0.01-.1		1-10

\*Spectrochemical analysis only

and C glasses were practically identical. The differences in the  $q_{ij}$  and  $p_{ij}$  which are reported arise from differences in the elastic moduli which data are needed in the calculations of the photoelastic constants.

#### Thermo-Optic Data

An optical interference method has been used to determine the change in refractive index with temperature from 25°C to 300°C for three neodymium-doped glasses. These are the samples B, C, and D. The results are shown in figures 1, 2, and 3 respectively. It can be seen in figures 1 and 2 that each of the samples B and C show a minimum in the temperature-refractive index curve. In the case of sample B the greatest change is only about  $1 \times 10^{-4}$  and the refractive index at 300°C is almost the same as at room temperature. With sample C, there is a change of almost  $4 \times 10^{-4}$  from the initial value to the minimum, and the value at 300°C is lower than the room temperature value by about 2.5



$\times 10^{-4}$ . The sample D glass shows a continuous decrease refractive index, the overall change being about  $4 \times 10^{-4}$ . The shape of the curve indicates that there is probably a minimum somewhere above  $300^{\circ}\text{C}$ .

### Thermal Expansion

The linear thermal expansion of samples B, C, and D has been measured, and the results are shown in figure 4. The curves for the samples B and C almost coincide, and, for the temperature range  $0^{\circ}\text{C}$  to  $300^{\circ}\text{C}$ ,  $\alpha = 10.65 \times 10^{-6}$  for either glass. The sample D glass exhibits a somewhat steeper curve, and, for the same temperature range,  $\alpha = 11.88 \times 10^{-6}$ .

### Density

The densities of two glass samples were determined by the buoyancy method using water as the immersion liquid. The values found were:

<u>Glass Sample</u>	<u>Density, g/cm<sup>3</sup></u>
D	2.6206
F	2.5490

### Elastic Constants

The elastic constants of two glass samples were determined by George Dickson, Dental Research Section, using a pulse echo technique. The values were:

	<u>Sample D</u>	<u>Sample E</u>
Young's Modulus, E, Newtons/m <sup>2</sup>	$6.58 \times 10^{10}$	$9.08 \times 10^{10}$
Shear Modulus, G	$2.66 \times 10^{10}$	$3.62 \times 10^{10}$
Bulk Modulus, K	$4.16 \times 10^{10}$	$6.14 \times 10^{10}$
Poisson's Ratio, $\gamma$	0.236	0.255

### Thermal Conductivity

Values for thermal conductivity of sample E glass at  $0$  and  $100^{\circ}\text{C}$  were given in our last report to the sponsor covering the period July 1 - December 31, 1968. Since there appeared to be a discrepancy between our results at  $0^{\circ}\text{C}$  and those of others on this laser glass, a second set of measurements was made. The results of both sets were:

Set	Temperature, °C	Thermal Conductivity Wm <sup>-1</sup> °C <sup>-1</sup>
1	5.91	1.21 <sub>6</sub>
1	104.78	1.35 <sub>2</sub>
2	5.95	1.20 <sub>3</sub>
2	45.47	1.28 <sub>3</sub>

The two measurements near 6°C differ by about 1.1%, well within the expected error of about two percent. To obtain smoothed values at 0, 50, and 100°C, the two points near 6°C were averaged, and a parabola was fitted to this point and the two points near 45 and 105°C. The results for the smoothed thermal conductivity values are:

Temperatures, °C	Thermal Conductivity Wm <sup>-1</sup> °C <sup>-1</sup>
0	1.19 <sub>7</sub>
50	1.29 <sub>0</sub>
100	1.34 <sub>8</sub>

#### References

- [1] J. B. Wachtman, Jr., W. E. Tefft, D. G. Lam, Jr., and R. P. Stinchfield, J. Res. NBS 64A (Phys. and Chem.) No. 3, 213 (1960).
- [2] F. Pockels, Wied. Ann. 37, 151 (1889): Lehrbuch der Kristalloptik (B. G. Teubner, Leipzig and Berlin, 1906).
- [3] R. S. Krishnan, Progress in Crystal Physics, Volume I (Interscience Publishers, New York, London, 1958).
- [4] H. Mueller, Phys. Rev. 47, 947 (1935).
- [5] F. Pockels, Ann. Phys. (Leipzig), 11, 726 (1903).

#### 3.6.2. CRYSTAL DEFECT STUDIES ON LASER MATERIALS

R. F. Blunt, T. Chang, and T. Tsang

Inorganic Materials Division  
Institute for Materials Research

#### Objectives

This investigation is a study of the causes responsible for degradation of performance of solid state lasers. The

effort has been redirected to consist of a study of "orange" degradation of laser ruby, by EPR and optical means.

#### Technical Approach

Experimental measurements consist mainly of optical absorption spectra and electron paramagnetic resonance on a variety of "ruby" samples. The following outline is being used:

1. Detailed spectra taken on undamaged "laser quality" ruby is to be compared with corresponding spectra on "orange" degraded samples.

2. Spectra will be examined for evidence of trace impurities, and, in the case of "orange" ruby, typical EPR crystal defect spectra that correlates with the orange coloring bands. It is noted that Stickley et al [1] suggests that the discoloration in laser rods may arise from color centers created by the pumping light at defects initially present in the crystals.

3. Special attention will be given to the detection of  $\text{Cr}^{2+}$  and/or  $\text{Cr}^{4+}$  ions that may exist in the orange samples.

4. A number of "doped" sapphire crystals are grown and studied. These include: rubies covering a wide range of Cr concentration; crystals containing single metal impurities; and several samples of "double doping" with Cr and one other metal.

5. Most crystals are colored by radiation with 50 KV x-rays and the resultant damage studied.

#### Experimental Results

Most of the samples employed were cut from Verneuil crystals grown in this laboratory. Metallic dopant impurity concentrations quoted are either nominal "starting material" values, or, as in the case of Cr, determined optically by the optical absorption method described by Dodd, Wood, and Barnes [2].

Ruby samples of various Cr concentrations were prepared, the optical absorption was measured, and then the crystals were colored by 50 KV x-rays and re-measured. The added coloration is seen to reach a maximum or saturation value with increasing irradiation.

Figure 1 is a plot of a typical sample of 0.076 mol %  $\text{Cr}_2\text{O}_3$  ruby. The top curves are the well known polarized spectra taken before irradiation. The bottom curves are plots of the added absorption at saturation, all plotted vs. wavelength. A simple reflection loss correction is made and the ordinate plotted as absorbance per cm sample thickness. On the bottom is the added x-ray coloration produced in a "pure" sapphire prepared from the same  $\text{Al}_2\text{O}_3$  powder used to grow the rubies.

A piece of commercial laser quality pink ruby was similarly examined and yielded similar data. The orange coloration produced by the irradiation consists of a broad band peaking near  $0.46\mu\text{m}$ , and a very strong band (or bands) at shorter wavelengths. Our principle attention has been focused, so far, on the  $0.46\mu\text{m}$  band.

Data taken on a large number of rubies verify that the coloration saturates with irradiation in a manner analogous to the familiar color center growth curves. There is also some evidence that the coloration exhibits a maximum when plotted as a function of Cr. concentration. These results have been reported by Novothy and Spurny [3], while coloration bands shown in figure 1 have been observed by a number of authors.

A brief search was made for possible impurity involvement in the coloration, by doping "pure" sapphire with a number of single metallic impurities. Included were V, Mn, and Ti, all presumably substitutional as trivalent ions. The absorption spectra were similar to that reported by

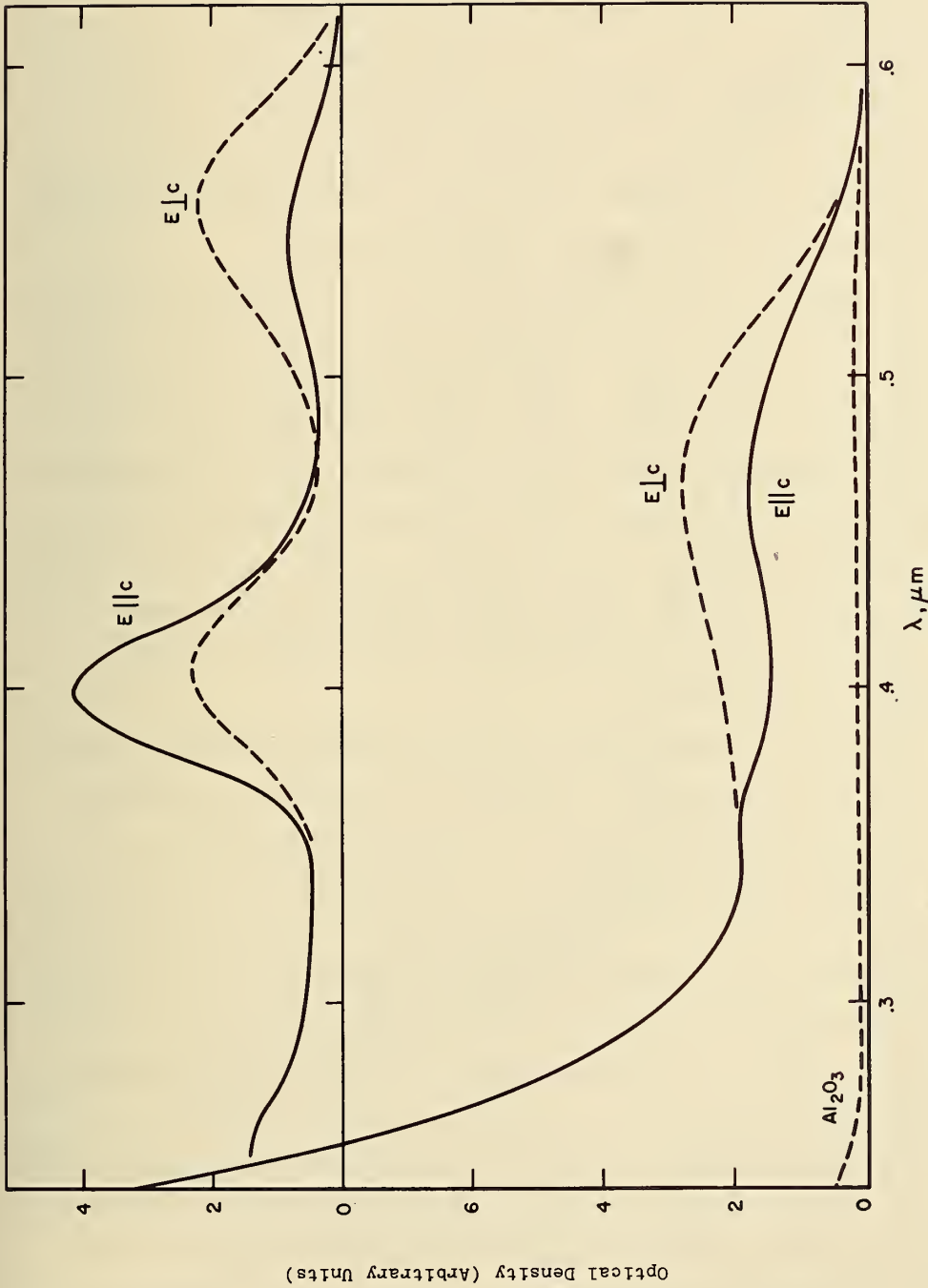


Figure 1. Optical absorption of 0.076 mole % ruby.  
 Top curves, absorption before irradiation  
 Center curves, added absorption induced by x-ray  
 Bottom curve, added absorption in "pure"  $\text{Al}_2\text{O}_3$   
 (Details in text)

McClure. [4] Irradiation produced added coloration, and samples were found to damage more easily than the undoped sapphire, but the absorption bands were observed only in the ultraviolet.

Double doped samples were studied in which single metals were added to ruby. One example, Mg + Cr, is of interest. Magnesium, presumably present as  $Mg^{2+}$ , could possibly result in either oxidation of  $Cr^{3+}$  to  $Cr^{4+}$  or oxygen vacancies or perhaps even both. These crystals were orange and optically resemble irradiated ruby.

Three sapphire crystals were grown to study the effect of Mg in greater detail. One crystal was doped with 0.025 mol % MgO and was colorless. The second crystal doped with 0.003 mol %  $Cr_2O_3$  yielded the expected  $Cr^{3+}$  spectra. The third crystal was doped with both Mg and Cr in like amounts.

Figure 2 summarizes the optical measurements on the second and third crystals. The bottom curve is the Cr doped crystal; the middle curve the double doped crystal as initially grown; and the top curve is the double doped crystal after irradiation.

The coloration resulting from Mg doping appears to be similar to that produced by irradiation without the magnesium. The limited additional effect of irradiation in the double doped sample suggests a  $Cr^{4+}$  model in which case essentially all of the  $Cr^{3+}$  was oxidized. An obvious difficulty with this is the apparent requirement of a very large oscillator strength for the presumed maximum possible  $Cr^{4+}$  concentration. Thus a trapped hole or electron, i.e., color center model would be more desirable in this respect.

Electron paramagnetic resonance measurements have been made on most of the ruby crystals that were studied optically. Comparison pieces cut from the same crystals were used. Measurements were made before and after irradiation.

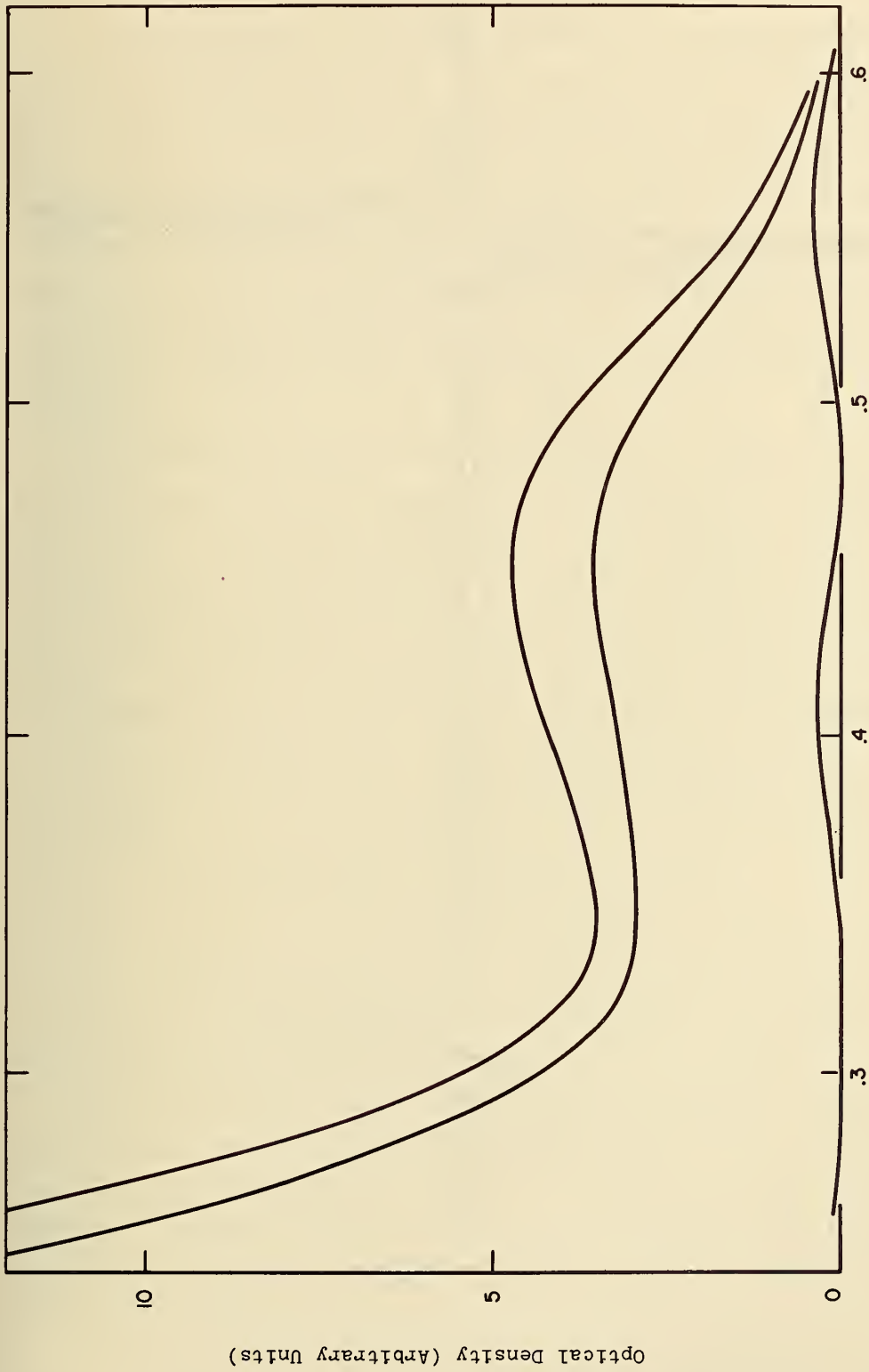


Figure 2. Optical absorption of Mg-doped ruby.  
 Bottom curve, .003 mole % ruby (no Mg)  
 Top curves, absorption in Mg-doped ruby before  
 and after irradiation  
 (Details in text)

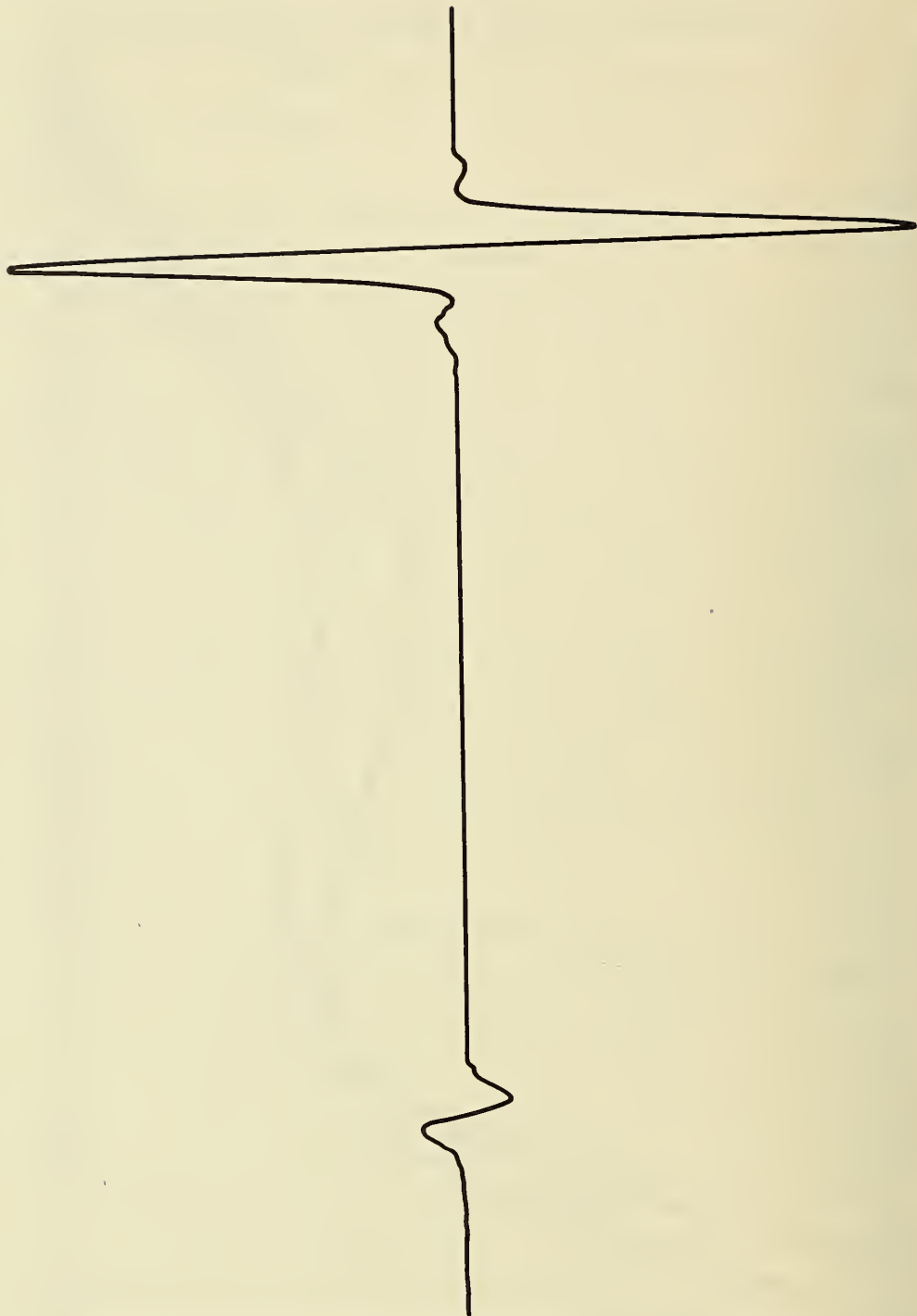


Figure 3. The EPR line of  $\text{Cr}^{3+}$  in ruby  
Large line  $-1/2$  +  $3/2$  transition  
Small line  $-1/2$  +  $1/2$  forbidden transition



It was hoped that extra lines or obvious readily recognizable changes in normal  $\text{Cr}^{3+}$  spectra would be found and correlated with the accompanying optical data. However, only typical  $\text{Cr}^{3+}$  spectra have been observed to date. A general systematic search for extra lines attributable to foreign paramagnetic impurities or to trapped holes or electrons present in paramagnetic configuration was made. Special attention was paid to the region where Hoskins and Soffer [5] report a line in orange ruby that they attribute to  $\text{Cr}^{4+}$ .

The sensitivity of the apparatus as used on the magnesium doped ruby of figure 2 is illustrated in figure 3, where two of the lines are seen. This sample could, of course, have  $\text{Cr}^{4+}$  ions even if the coloration were due to some other mechanism. The spectrometer operates at X-band frequencies, and the sample was at 4.2K. The magnetic field was approximately parallel to the C-axis of the ruby. From the measured values of B, and the calculations of du Bois [6], the large line is the  $-1/2 \longleftrightarrow +3/2$  transition near  $B + 0.34$  Tesla with a  $g_{\text{eff}} + 1.9955$  and a line width of about  $2 \times 10^{-3}$  Tesla. The small line is from the forbidden  $-1/2 \longleftrightarrow 1/2$  transition near  $B + 0.39$  Tesla, which is seen by virtue of a slight crystal misalignment. The curve shown is a copy of the recorder chart paper and illustrates the signal to noise ratio available during the search for new lines.

The apparent lack of obvious paramagnetic "defects" in the orange rubies is rather surprising, as is the lack of any observable change in the  $\text{Cr}^{3+}$  spectra after coloration. However, efforts to observe either or both of these are continuing. Optical pumping on samples at low temperature will be further explored.

A new optical EPR cavity is under construction that will permit non-destructive resonance studies on laser rods down to very low temperatures.

The optical studies on x-ray irradiated rubies having special dopings will be continued. The evidence presented by Stickley [1] that the optically pumped coloration is different from x-ray coloration would make mandatory the study of samples colored by optical pumping.

This will be done when rubies that are easily damaged by "pumping" light become available.

#### References

- [1] C. M. Stickley, H. Miller, E. E. Hoell, C. C. Gallagher and R. A. Bradbury, J. Appl. Phys. 40, 1792 (1969).
- [2] D. M. Dodd, D. L. Wood, and R. L. Barnes, J. Appl. Phys. 35, 1183 (1964).
- [3] J. Novothy and Z. Spurny, Czechoslovak Jour. of Phys. 16B, 119 (1966).
- [4] Donald S. McClure, J. Chem. Phys. 36, 2757 (1962).
- [5] R. H. Hoskin and B. H. Soffer, Phys. Rev. 133, A490 (1964).
- [6] E. O. Schulz-duBois, Bell System Tech. J. 38, 271 (1959).

### 3.6.3. EXAMINATION OF RUBY LASER RODS BY X-RAY DIFFRACTION TECHNIQUES

E. N. Farabaugh and F. A. Mauer

Inorganic Materials Division  
Institute for Materials Research

#### Objective

This study was undertaken to determine whether x-ray diffraction techniques may be used to characterize ruby laser rods. A correlation between crystal perfection and its performance in a laser was considered.

#### Approach and Results

Comparison of laser performance and crystal perfection has been carried out on three ruby rods. Dr. John Hall of the NBS Boulder Laboratories supplied the rods and evaluated their laser performance. Their performance was described as "Fairly Good" (rod A), "Medium to Poor" (rod B), and "Lousy" (rod C). The Laue back-reflection, Laue transmission and

pseudo-Kossel techniques were used in the x-ray examination to detect small-angle grain boundaries and c-axis wander.

By translating the rod in an x-ray beam and taking back-reflection films at points along the rod, it was determined that all rods had some c-axis wander. The magnitude was of the order of  $1/2$  to  $1\ 1/2^\circ$  for each rod. Examination of the individual diffraction spots showed some splitting in the case of each of the rods. This splitting probably indicates that the beam was incident on a subgrain boundary, but some of the observed splitting may be due to grinding done in fabricating the rods.

Back-reflection Laue films were also taken across the end faces of all three rods. Rod A yielded the best Laue films and rod C yielded the worst Laue films. Those for rod B were somewhere between those for rods A and C. The diffraction spots from one end of rod C were badly split and there was a variation in orientation of approximately half of a degree across the face of the rod. The other two rods had no misorientation across their faces. The structure of the spots was best for rod A and slightly poorer for rod B.

The pseudo-Kossel technique was also used to study the end faces of the rods. Analysis of the diffraction patterns taken by this technique gave results which were in agreement with those from the Laue back-reflection films. Both ends of rod A yielded pseudo-Kossel patterns which were sharp and had no discontinuities. One face of rod B gave a high quality pattern, while the opposite face gave a pattern with several discontinuities. One face of rod C gave a sharp pattern while the opposite face gave a very poor one.

Transmission Laue films were taken at three points along each rod. This technique samples a volume extending through the rod rather than a surface layer. Pictures taken in this

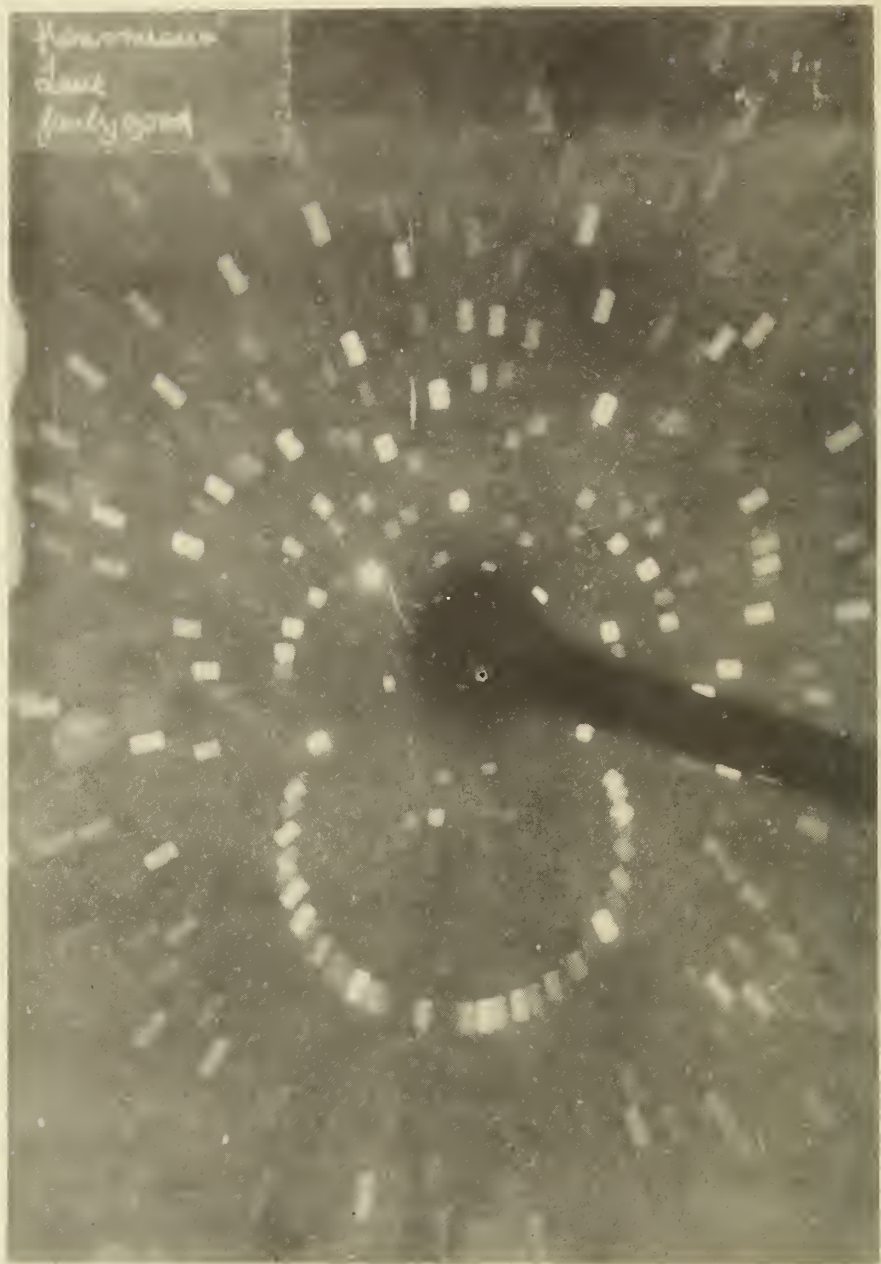


Figure 1. A transmission Laue pattern of rod A. The diffraction spots are only slightly split. All the transmission patterns for rod A were of good quality.



Figure 2. A transmission Laue pattern of rod C. The diffraction spots are so badly split that it is difficult to tell where one spot ends and the next begins. A pattern like the above arises when the x-ray beam passes through a volume of the crystal containing regions of differing orientation. All films of rod C were similar to the above.

manner revealed qualitative differences that were quite striking:

1. Well formed spots with only slight splitting were observed in the case of rod A (fig. 1).
2. Moderate splitting of spots was seen in one of the three pictures from rod B.
3. Extreme splitting of spots occurred in all three pictures from rod C (fig. 2).

Although the x-ray examination did reveal differences between rods A, B, and C that correlated qualitatively with laser performance, these techniques have not been applied to the differentiation of high performance rods. Better rods are being obtained, and an attempt will be made to modify the techniques which are required to classify these rods.

#### 3.6.4. LASER INDUCED DAMAGE STUDIES

N. N. Winogradoff, A. H. Neill, Jr., and J. Mitchell

Inorganic Materials Division  
Institute for Materials Research

##### Objective

The objective of this work was to:

1. Devise techniques for comparing the energy and power damage thresholds for various samples of laser glasses,
2. Develop an understanding of the damage mechanism, and,
3. Relate the bulk physical properties of the glasses to the above, with the aim of determining the optimum properties of glasses for very high power laser operation.

##### Approach

With the exception of consulting trips to other laboratories and relevant conferences, the work described below was charged to the STO of ARPA, and included:

1. Technical literature survey of laser damage work,

2. Serving as consultants in advising on the nature of the problem and in setting up a laser system capability for experimental work on laser glass damage,

3. Preliminary experimental work on long pulse and Q-switched beam characterization of a ruby laser,

4. Preliminary experiments on the comparison of the nature of the damage produced by focused long and Q-switched ruby pulses in glass and plexi-glass samples.

The visits to other laboratories and relevant conferences, charged to the Materials Office of ARPA, included The Conference on Lasers and Opto-Electronics, University of Southampton, England\*; The National Physical Laboratory, England\*; The American Optical Company, Massachusetts; and the ASTM Laser Glass Damage Symposium in Boulder, Colorado.

#### Technical Status Review

All the work we came across was carried out with focused laser beams. Both verbal consultations and the literature survey showed the field to be very confusing except for the fact that the (apparently intrinsic) laser induced damage can exist in two basic forms; (a) circular disc-like cracks, the distribution and orientation of which can be controlled by the application of an external stress, and (b) thin lines running parallel to the beam direction. The width of these lines can be so fine as to defy resolution of any structure within the line or wide enough to easily display a random "debris" type structure. In some cases, the damage exhibits localized clusters of type (a) cracks which may or may not be connected by type (b) lines.

A third type of damage related to the presence of absorbing inclusions results in a "star-burst" type of locali-

---

\*We refer the reader to the trip report, which is in the appendix, for details.

zed cracking. With improved, platinum free samples of glass this type of damage is almost extinct and will not be considered in this report.

There appear to be at least three distinct mechanisms responsible for the damage, (a) localized heating (or energy absorption), (b) multiphoton ionization and subsequent acceleration of the free electron to destructive avalanching energies, and (c) electrostriction resulting in self-focusing and acoustic effects.

By using two identical short pulses with a separation of some 100 $\mu$  sec, it was shown that preheating of the focused region by the first pulse did not reduce the damage threshold energy density for the second pulse, and it was concluded that the damaging factor was the power rather than the energy content of the beam [1]. In contrast with this experiment, the same authors found that an increase in the over-all temperature of the sample reduced the destruction threshold [1].

They also found strong similarity in the damage produced in sapphire by both neodymium and ruby laser pulses and also found that the frequency doubled beams from these lasers yielded damage thresholds which were constant over a temperature range from 77°K to 700°K, and that the damage due to these higher photon energies was mainly in the form of very thin long lines as distinct from the circular disc-type fracture observed with the Q-switched fundamental frequencies.

They also found a linear relationship between the energy density (joules per square centimeter per pulse duration) for damage and the pulse width (at constant power). The extrapolation of this curve suggests that the damage threshold would be reduced to zero at vanishingly small pulse durations (pico second pulses). This experimental evidence appears to be contrary to common belief.



## Technical Report

Because of the relative ease of preparing polished blocks of plexiglass, we compared the nature of the damage produced with ruby laser beams focused by a  $\approx 10$  cm focal length lens in glass and in methyl methacrylate blocks.

Visual and microscopic examination did not reveal any difference in the nature of the damage in these two materials which always exhibited the disc-like cracks with long pulse excitation and thin  $\approx 1$  mm x 5 cm long tracks with 30 n sec Q-switched pulses having energy contents of  $\approx 25$  and 3 joules, respectively.

These experiments showed that preliminary setting-up, optical alignment, and focusing of glass damage experiments could be easily and economically established with plexiglass blocks in such a way that the scarce experimental glass blocks can be conserved for damage studies when the system had been optimized on the methyl methacrylate samples.

All our long pulse mode experiments yielded similar disc-like cracks in the glass and methyl methacrylate blocks and showed that this type of damage was limited to the upstream side of the focus.

The Q-switched pulses invariably yielded the thin long tracks, described above, which passed through the focus without highlighting the focal point. This result contrasts with the thin tracks observed by Edwards [2], only on the upstream side of his focal point.

Both types of damage were luminescent during formation, and it has been suggested that the emission could be due to high temperature incandescence. Assuming black body emission, temperatures of  $>10^6$ °K have been calculated. However, it is difficult to correlate these temperatures with the apparent temperature dependence of the damage threshold where a few °K can apparently produce a marked difference.

Since the track-like damage is almost certainly a form of self-focusing process, it would be expected to be dependent on the degree of initial focusing of the beam, essential to produce damage, by "normal" laboratory laser systems.

For this reason, more significant quantitative measurements could be obtained by using collimated beams where the required energy densities could be obtained by optical reduction of the beam width. However, under these circumstances, surface damage having a lower threshold may set in before the radiation could produce bulk damage so that an optimum degree of convergence in thick samples will have to be determined for the evaluation of  $\alpha$  the bulk damage threshold.

J. Mitchell is currently re-designing and constructing a holder for the bi-planar phototube with improved impedance matching which should result in response times of better than 230 pico seconds for power measurements of the pulses used in the damage studies, and A. H. Neill's calorimeter is being recalibrated and evaluated for pulse energy measurements in Boulder.

#### References

- [1] G. M. Zverev, T. N. Mikhailova, V. A. Pashkov, and N. M. Solov'eva, Soviet Physics JETP 26, p. 1053 (1968).
- [2] N. N. Winogradoff, Trip report covering attendance at the Laser and Opto-electronics Conference, Southampton and the National Physical Laboratory, March 1969.

### 3.6.5. CHARACTERIZATION STANDARDS FOR LASER MATERIALS

J. L. Torgesen

Assisted by the following staff in the Analytical Chemistry Division: B. A. Thompson, E. Miller, Virginia C. Stewart, T. A. Rush, T. C. Rains, E. R. Deardorff

Inorganic Materials Division  
Institute for Materials Research

#### Objectives

1. To develop precise methods for the chemical analyses of solid laser materials to include determinations of major constituents and trace quantities of impurities.

2. To provide characterization of laser materials as to physical defects and dislocations.

#### Approach and Results

##### Trace Quantities of Impurities in Ruby

Neutron activation analysis was used for the determination of trace elements in specimens cut from three different ruby boules. The three ruby boules were doped with  $\text{Cr}_2\text{O}_3$  at nominal levels of 0.05%, 0.075%, and 0.10%, respectively. Two specimens, cut from opposite ends of each boule, were analyzed.

Each sample (200-800mg) was sealed in polyethylene and irradiated for 30 minutes in pneumatic tube RT-3 of the NBS Reactor at a power level of 5 MW ( $3 \times 10^{13} \text{ n} \cdot \text{cm}^{-2} \cdot \text{sec}^{-1}$ ). A copper flux monitor was taped to the outside of each capsule. After irradiation the samples were allowed to decay to 30 minutes to reduce the activity of 2.3-minute  $^{28}\text{Al}$  from the  $\text{Al}_2\text{O}_3$  matrix. Since the ruby crystals could not be dissolved readily, all analyses were non-destructive. The crystals, after irradiation, were rinsed in alcohol and in 1:1  $\text{HNO}_3$  to remove surface contamination and were then counted with a 47-cc  $^3\text{Ge}(\text{Li})$  detector and a 2048-channel analyzer. Several counts were made at different times to permit observation of nuclides of short, intermediate, and

Table 1

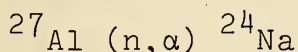
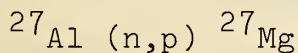
Results of activation analysis of ruby laser crystals, ppm  
Crystal designation

Element	050 (4)	050 (9)	075 (4)	075 (9)	100 (4)	100 (9)
Cr (% Cr <sub>2</sub> O <sub>3</sub> )	0.059	{0.072 0.065}	0.078	0.086	0.104	0.098
Ba	89	111	68	5.3	1.1	16
Sr	2.5	3.0	1.9	<0.1	<0.1	0.5
Cu	0.051	0.089	0.050	0.054	0.038	0.028
Co	2.22	1.49	3.08	3.95	0.125	0.104
W	0.29	0.19	0.55	0.15	0.41	0.60
Au	0.0028	<0.0008	0.0014	<0.001	0.0021	<0.0003
La	0.036	0.027	0.011	<0.003	<0.004	<0.008
Mn	0.0018	0.022	0.0023	0.0027	<0.001	<0.001
Ir	0.040	0.037	0.033	0.038	0.023	0.033
Ga	0.024	0.030	0.070	0.096	0.034	0.039

long half-life. The concentration of each element detected was determined by comparison with a standard composed of a known amount of the element, irradiated and counted under the same conditions as the samples.

The results obtained are shown in table 1. It can be seen that a number of elements were observed at the ppb level or above. We estimate, on the basis of previous experience, that the standard deviation in each case, except as noted below, is about  $\pm 5\%$ .

Although the aluminum activity produced by thermal neutrons in the  $\text{Al}_2\text{O}_3$  matrix has only a 2.3 minute half-life and thus does not interfere with the measurement of nuclides of longer half-life, two other isotopes are produced by the action of fast neutrons on the aluminum:



The  ${}^{27}\text{Mg}$ , with a half-life of 9.5 minutes, does not constitute a serious interference, but the  ${}^{24}\text{Na}$  has a half-life of 15 hours and, thus, can interfere with the measurement of all activities having half-lives shorter than 15 hours. To minimize this interference we irradiated the samples in the facility with the highest available ratio of thermal to fast neutrons. Even here, the magnitude of the sodium-24 "background" required large corrections for the Cr, Ga, Sr, and the low Mn activities and, therefore, the uncertainty for these values is probably poorer than  $\pm 5\%$ . This is particularly true for copper because, in addition to the high Compton continuum, or "background", the  ${}^{24}\text{Na}$  emits a small amount of 0.511 MeV radiation, which is the same energy as that from  ${}^{64}\text{Cu}$ . A very large correction was thus required for the copper values and, in fact, it would probably be safest to consider them as upper limits to the Cu concentrations in the crystals.

Within the next month or two we should have access to a terminal in the NBS Reactor with a much higher thermal-to-fast neutron ratio and so we should be able to obtain much better results for these shorter half-life nuclides. It is possible that we could also determine K, Rb, Ca, and Zn at the ppm level or below if this interference were removed.

#### Analyses of Nd-doped Glasses

Specimens of three commercially available Nd-doped laser glasses were analyzed by a qualitative spectrochemical method. The glasses are identified as samples B, C, and E. The results of this analysis are shown in table 2. It is apparent that the samples B and C contain mixed alkalis, and evidently are based on similar compositions. The sample E glass is of a much different composition and evidently is a lithium aluminum calcium silicate.

Data on the optical properties of the glasses, obtained on an associated project, bears out the fact that the sample E glass is of a different composition.

Based on the results of the spectrochemical analyses, precise determinations of the major constituents of the glasses were then made. The results are given in table 3, along with the method used for each element.

#### Future Work

Due to personnel changes the project on Characterization Standards for Laser Materials has been discontinued as of June 30, 1969. The work on chemical characterization will be continued under Project 3130423, Physical and Chemical Properties of Laser Materials.

Tasks that are underway or will be undertaken include:

(a) the determination of  $dn/dc$  for single crystal ruby. Refractive index measurements are now being made on ruby prisms doped at nominal levels of 0.03%, 0.05% and 0.064%  $Cr_2O_3$ . Determinations of the absolute concentrations of

Table 2. Spectrochemical analyses  
of three laser glasses

<u>Element</u>	<u>Glass Sample</u>		
	<u>B</u>	<u>C</u>	<u>E</u>
Al	0.1-1	0.1-1	1-10
B	<.001	<.001	<.001
Ba	1-10	1-10	.001-.01
Ca	.01-.1	.01-.1	1-10
Cu	<.001	<.001	-
Fe	.001-.01	.001-.01	.001-.01
K	1-10	1-10	<.001
Li	<.001	<.001	1-10
Mg	<.001	<.001	<.001
Na	1-10	1-10	.01-.1
Nd	1-10	1-10	1-10
Pb	1-10	1-10	-
Rb	.001-.01	.001-.01	-
Sb	.1-1	1-10	-
Si	>10	>10	>10
Ti	.1-1	.1-1	-

Note: >, greater than; <, less than,  
-, not detected: values given in  
percent composition by weight.

Table 3. Major constituents in three Nd-doped glasses

<u>Oxide</u>	<u>Composition - wt%</u>			<u>Analytic method</u>
	B	C	E	
SiO <sub>2</sub>	67.8	66.3	66.1	Gravimetric
Na <sub>2</sub> O	7.90	3.60	0.05	Flame Emission Spectrometry
CaO	0.04	0.02	10.1	Flame Emission Spectrometry
K <sub>2</sub> O	13.8	18.2	-	Flame Emission Spectrometry
Li <sub>2</sub> O	-	-	14.5	Flame Emission Spectrometry
PbO	1.10	1.75	-	Atomic Absorption Spectrometry
Al <sub>2</sub> O <sub>3</sub>	0.12	0.06	4.38	Flame Emission Spectrometry
Sb <sub>2</sub> O <sub>3</sub>	1.26	3.57	-	Atomic Absorption Spectrometry
Nd <sub>2</sub> O <sub>3</sub>	5.49	3.42	3.19	Solution Spectrometry
Fe <sub>2</sub> O <sub>3</sub>	0.007	0.009	0.006	Solution Spectrometry
TiO <sub>2</sub>	0.19	0.39	-	Solution Spectrometry

Cr in the specimens will be made and the data correlated with refractive index.

(b) the determination of Cr<sup>+3</sup> absorption coefficients in ruby and the correlation with absolute concentration.

(c) completion of the analysis of commercially-made Nd-doped glasses.



### 3.6.6. STUDIES ON TECHNIQUES TO DETECT PLATINUM INCLUSIONS AND TO MEASURE ND-GLASS QUALITY BY LIGHT SCATTERING

Herbert S. Bennett

Inorganic Materials Division  
Institute for Materials Research

#### Objective

To determine whether dielectric relaxation, NMR, and light scattering capabilities, for which NBS has at present the equipment and the personnel may be employed for the study of inclusions in Nd-glass and for quality tests of Nd-glass.

#### Technical Information

Feasibility studies on two techniques by which one might hope to measure the size, shape, and concentration of platinum inclusions in Nd-glass were considered. The dielectric relaxation experiments, which are based upon the Maxwell-Wagner dispersion, measure the conductivities and the permittivities of a suspension (platinum in Nd-glass for example) as a function of frequency. The suspension is viewed as electrically equivalent to a simple resistance-capacitance network. The dispersion frequency for Pt in Nd-glass is estimated to be about  $10^{16}$  Hz and the change in resistance and capacitance to be about one part in  $10^6$ . Such high frequencies and small changes in resistance make this method unsuitable for Pt detection in Nd-glass.

The conventional NMR (nuclear magnetic resonance) techniques are estimated to be insensitive to the concentration of Pt inclusions which are expected, even when methods to increase the signal to noise ratio are employed, such as using high magnetic fields, low temperature, and time averaging. However, one should not conclude that all magnetic resonance techniques will be unsuccessful in detecting Pt inclusions. The complicated double resonance techniques, the combination of optical and microwave resonance techniques, and ENDOR

experiments might prove successful. But, each of the latter will lead only to a research project and not to analytic techniques which are applicable to many materials.

Light scattering experiments were performed on two Nd-glass rods (sample F, 2.54 cm in diameter by 5.08 cm long). One sample was rated excellent and the other was rated as less than excellent but not poor either. The ratings are based upon examining the white light from a projector which is scattered at  $90^\circ$ . Seed-and-gas-bubble inclusions have little change in brightness as the sample is rotated. Large enough Pt inclusions exhibit an easily observed change in brightness upon rotation of the sample. The ratings were given by the supplier of sample F. A light scattering photometer was used for these experiments. The intensity of light scattered from  $30^\circ$  to  $150^\circ$  in the azimuthal plane (the plane which is perpendicular to the axis of the rod) was measured for the 546 nm and the 436 nm lines of a mercury arc lamp. The scattering intensity as a function of scattering angle for both vertical and horizontal polarizations of the incident light showed no difference between the two samples. The negative results may be due to the fact that the light source (mercury arc) and detector (photo-multiplier tube) are not stable enough to distinguish passively between excellent and good samples of Nd-glass. They also suggest that if information on rod quality is available in the light-scattering data it is probably contained in the forward ( $0^\circ$ ) and backward ( $180^\circ$ ) scattering directions. One should not conclude however that light scattering measurements are not sensitive enough. Perhaps, more sophisticated equipment using He-Ne lasers and vacuum photo diodes might provide the answer. The writer acknowledges and thanks Dr. Lois Frolen and Mr. Given W. Cleek for performing the above light scattering experiments and for the sample preparation.

3.6.7. APPENDIX  
SUMMARY FOREIGN TRIP REPORT

Report by:

Nicholas Winogradoff, Research Physicist  
Solid State Physics Section (313.07)  
Inorganic Materials Division, IMR  
National Bureau of Standards

Locations Visited:

24 March 1969 - 28 March 1969	University of Southampton Southampton, England
31 March 1969	National Physical Lab Teddington, Middlesex England

Purpose of Trip:

- (a) To attend a Joint Conference on Lasers and Opto-Electronics sponsored by the Institution of Electronic and Radio Engineers, The Institution of Electrical Engineers (Electronics Division), The Institute of Physics and Physical Society, The Institute of Electrical and Electronics Engineers, and the University of Southampton, with the specific purpose of learning the latest state of the art in laser glass damage problems and study procedures, and laser glasses in general.
- (b) To establish contact with others working on semi-conductor injection lasers, and other related fields. Being international, and having 122 contributing authors drawn from countries including France, Germany, India, Japan, Switzerland, U.K., U.S.A., and U.S.S.R., this conference was particularly well suited for the above purposes.

Trip Summary:

Although we were particularly interested in the damage properties of neodymium-doped glass, the main paper relating to laser glass damage was given by Mr. J. G. Edwards of the

National Physical Laboratory, and this work was related to the elucidation of damage mechanisms rather than the comparison of various glasses.

I was interested in the French attitude to research in general, and introduced myself to some of the French delegates attending the meeting, and was most impressed by their friendliness. Two of them, Drs. Jean Michel Jego and Lain Ternaude were active in laser glass damage problems and gave me reprints of some of their work relating to studies of the changes in the refractive index of glass samples subjected to focused laser beams and the generation of giant pulses in small samples of material by focused optical pumping respectively. The latter produced  $375\text{MW}/\text{cm}^2$  pulses having half widths of the order of 1 nanosecond out of samples measuring about 4 mm in length.

The refractive index studies were based on an extension of Bell and Landt's work in water (reported by Dr. Bennet), and included the use of direct and Schlieren photography, the latter proved to be the more informative. Dr. J. M. Jego had written a thesis on the study of laser damage in glasses - this represented a comprehensive volume of work.

The rest of the summary given below will be restricted to the actual proceedings of the conference.

While in Southampton, I also had most interesting and instructive discussions on band tailing in gallium arsenide with Dr. G. H. B. Thompson, whom I had met on a previous visit to the Clarendon Laboratories, Oxford University. These discussions will be continued by mail.

The Russian papers on semiconductor lasers were very poorly presented and lacked clarity in objective and design.

Conference Proceedings:

(1) J. G. Edwards, National Physical Laboratories.

Laser-Amplifier Source used in Damage Studies

The laser source used, consisted of an auxiliary oscillator feeding an unusual amplifier which consisted of a  $\text{Nd}^{3+}$  sample B glass block, measuring  $\approx 10 \times 10 \times 1$  cm sandwiched between pumping flash lamps. Following initial amplification in passing through a strip of this block, measuring 0.118 cm in height, 1.0 cm in width, the beam was deflected by a tilted block of fused silica spinning at  $\approx 411$  herz, (serving as a Q switch) forced into the  $\text{TEM}_{00}$  mode by rectangular diaphragms formed out of fused silica rods, and reflected back through the spinning block of quartz into another strip of the amplifying block, having the same dimensions as given above, but displaced some 0.148 cms below the former.

This displacement was governed by the speed of rotation of the block and the external optical path length. The beam was then successively swept through different layers of the block which thus served as a compact series of amplifier rods, and after some 56 amplifying passes, the beam traversing the lowest "strip" of the block was deflected out.

The system used enabled the pulse half widths to be varied from 2.9 ns to 80 ns by placing suitable glass fiber grids between the input face of the amplifier block and a mirror. An amplification coefficient of  $0.07 \text{ cm}^{-1}$  was obtained and this resulted in a gain of 4 for each double pass through the block. The energy density in the slab was  $16.5 \text{ J/cm}^2$  and was claimed to be well below the fracture energy density of the glass  $30\text{-}100 \text{ J/cm}^2$ .

(2) J. G. Edwards, National Physical Laboratory. Laser Damage Mechanisms in Glasses

The above  $1.06 \mu\text{m}$  diffraction limited Q-switched pulses having pulse widths ranging from 3-60 ns with powers up to

100 MW were focused into the volume of various glass samples.

The peak powers were measured by means of biplanar photo emissive diodes contained in special modified containers where impedance matching for the output was obtained by tapered co-axial shaping techniques. This procedure was claimed to shift the response time for the wide area detector to  $\approx 250$  pico seconds.

The energy in the beam was computed from the pulse shape displayed on an oscilloscope and claimed to be known to 7% absolute accuracy. (The writer has considerable misgivings about this technique and its ability to produce energy measurements to this accuracy, but there does not seem to be any better way of making such measurements at the present time). Energies entering and leaving the sample were measured and the absorbed energy deduced. A plot of absorbed energy against input energy was made. The energy threshold for damage was given by the value of input energy for which an extrapolated portion of this curve intersects the input energy axis.

Visually, most of the damage produced by the focused beams was in the form of very thin "hair lines" about  $1 \mu\text{m}$  in width and several centimeters in length. A plot of the square of the length,  $l^2$ , against the incident energy was also a straight line whose intercept on the energy axes also gave a corresponding energy threshold for damage. These linear plots and the fine line structure of the damage usually observed suggested that they were of intrinsic nature.

Occasional large deviations from the linear plots were taken to indicate a different damage mechanism due to inclusions but even in large samples of laser glass B these were rare. Typical energy threshold levels for the "intrinsic" damage were  $1.5\text{J}/\text{cm}^2$  for 50 ns pulses  $30\text{ Mw}/\text{cm}^2$ , and  $100\text{J}/\text{cm}^2$  for 3 ns pulses  $\approx 33\text{ GW}/\text{cm}^2$ . When surface damage was

observed, the threshold energies were a factor 3 lower. The above pulse length dependence suggested that the pico second pulse component often observed in Q-switched lasers may not contribute to the damage threshold.

By screening a side viewing photo detector from the scattered  $1.06 \mu\text{m}$  radiation, Edwards showed that each damage track emitted "white" light during its formation and suggested that the damage was due to plasma formation initiated and propagated by multiphoton freeing of an electron and its subsequent acceleration by the E field in the radiation. Recent work by Russians showed that x-rays could be emitted from such plasma in gases and these could be used to estimate temperatures in the plasma. Temperatures in excess of  $10^6 \text{K}$  have been calculated.

Basing his arguments on this model, Edwards suggested that the energy threshold for damage should be increased by the incorporation of electron traps in the glass. Such an effect was apparently observed in ruby doped with  $\text{TiO}_2$ , in Germany, where, at high  $\text{TiO}_2$  contents the energy threshold for damage was increased by a factor of 45.

(3) G. H. B. Thompson, Standard Telecommunication Laboratories, Ltd., Harlow, Essex, Injection and Recombination of Carriers in GaAs Electro-Luminescent Diodes Below Threshold

Examination of the spectral output and lifetimes of the injected electrons in a p-n GaAs junction made by diffusing Zn into an Si doped material indicated the presence of two distinct lifetimes, one of which is quadratic and the other linear with current. The lifetimes were said to depend on the part of the junction examined, the latter being dominant in the p-type side further away from the junction.

(Writer's comment: Since Si is known to be amphoteric, it was a pity that this dopant was used in the n-type side of the diode, as the two lifetimes may be due to differences in

recombination cross sections for the two types of acceptors.)

Thompson attributes a low mobility to the electrons lying in the low energy states in the tail of the conduction band. From our point of view, it is particularly interesting to note that he finds evidence of a distinct energy step of the order of 0.01 eV associated with marked changes in electron mobility -- this adds further evidence to our contention of the existence of a "discrete" energy level lying close to the conduction band.

(4) H. R. Whittman, U. S. Army Missile Command, Alabama, Temperature Effects in GaAs Lasers

This paper described the performance of GaAs p-n junctions formed by solution regrowth, over a temperature range extending "below 50°K to above 100°K". The nature of the diodes was not well defined and the interpretation of the results in terms of conduction band tailing with radiative recombination to a "discrete" state near the valence band edge lacked direct experimental evidence. A comment by Burrell of STL Ltd. indicated that the latter had evidence for exponential tailing at both band edges. Whittman and I have discussed the problem of band tailing at some length and are now engaged in further discussions by mail. We hope that mutual laboratory visits will take place shortly.

(5) A. R. Goodwin, Standard Telecommunication Laboratories, Ltd. Harlow, Essex, Cooled and Room Temperature GaAs Lasers

Efficiencies up to 50% for Zn diffused GaAs laser diodes at 77°K and up to 15% at 300°K have been reported. Although efficiencies of 35% were observed by using solution regrown n-type material as a substrate for the Zn diffusion and the switch on delay times observed with these lasers could be reduced by suitable heat treatment, problems with short pulse operation were still to be solved.



(6) J. R. Peters and C. E. E. Stewart, Standard Telecommunication Laboratories, Ltd. Harlow, Essex, Ga(AsP) Visible Lamps and Arrays

The diodes were generally formed by Zn diffusion into layers of  $\text{GaAs}_x\text{P}_{1-x}$  produced by vapour phase epitaxy on to GaAs substrates using arsenic and phosphorous trichloride predoped with Se or S. In some cases, mixed arsine and phosphine were used for the formulation of the n-Ga  $\text{As}_x\text{P}_{1-x}$  layer.

A compact 5x7 alphanumeric array of  $\text{GaAs}_x\text{P}_{1-x}$  diodes (retaining direct band gap characteristics) was demonstrated. (it was a pity to note that no attempt was made to improve the efficiency for the power output by controlled compensation.)

Visit to Mr. J. G. Edward's Laboratory, National Physical Laboratory, Middlesex:

This visit proved to be particularly fruitful, as I was able to see the actual nature of the damaged glass. A particularly interesting aspect of this was that all the samples I saw indicated that using focused Q-switched Nd laser flashes caused damage in the form of hair line tracks originating at or near the focus and extending several centimeters upstream. No bubbles could be resolved under the microscope and there was no evidence of scattered debris or damage areas as seen in the damage tracks we generated by focusing Q-switched 30ns ruby pulses in glass.

In a quantitative evaluation of glass it is, of course, essential to correlate the damage and beam characteristics, and the latter has to be specified with the best possible precision. Since the Q-switched pulses can vary from shot to shot, each individual pulse was measured by a special beam splitter feeding a small fraction of the beam into a biplanar photo emissive detector. Edwards has done very extensive work on beam measurement and characterization and

his methods may well be regarded as a standard for the present state of the art.

Using special tapered coaxial connectors, drawings of which were given to me, Edwards was able to decrease the response time to some 250 pico seconds and demonstrated that this was a considerable improvement on the standard housing.

A copy of Edward's beam splitter and detector system is now being constructed and will be used in our damage work.

#### TRIP REPORT

Report by:

Herbert S. Bennett  
Physical Properties Section 313.05  
Inorganic Materials Division, IMR  
National Bureau of Standards

Locations and Persons Visited:

7 June	Dr. E. C. Crittenden Physics Department Navy Postgraduate School Monterey, California
9 June	Prof. S. Harris Microwave Laboratory Stanford University Palo Alto, California
10 June	Dr. J. Swain Lawrence Radiation Laboratory Livermore, California
11 June	Dr. H. Winston and Dr. C. Giuliano Hughes Aircraft Research Labs. Malibu, California
12 June	Dr. A. Keig Union Carbide (Linde) San Diego, California
16 June	Dr. G. Gobeli and Dr. E. Jones Reactor Building Sandia Corporation Albuquerque, New Mexico

17 June Dr. P. Avizonis and Capt. Abela  
Air Force Weapons Laboratory  
Kirtland Air Force Base  
Albuquerque, New Mexico

18 June Prof. D. Edwards  
Physics Department  
Colorado State University  
Fort Collins, Colorado

19 & 20 June ASTM - Subcommittee II on Lasers  
and Laser Materials  
National Bureau of Standards  
Boulder, Colorado

Purpose of Trip:

(a) To visit representative laboratories associated with universities, government installations, and industries which have experienced damage or degradation in systems containing lasers and laser materials.

(b) To establish contact with researchers at these laboratories in the fields of high power pulsed lasers, laser materials, and non-linear optics.

(c) To learn the materials problems which the above researchers have encountered and how they have overcome them or how they have managed to accommodate them when practical solutions were not possible. Also, to attempt to learn the type of problems which are not discussed in the published literature.

(d) To investigate possible areas of laser damage research in which the National Bureau of Standards might make a unique and definitive contribution within the limitations of its present resources.

This report contains two sections. The first section is a summary of the writer's views on current laser research and on its problems in the United States. The second section contains brief accounts of the technical information obtained from each of the laboratories listed above.

## Summary and Subjective Comments:

One of the current topics among laser researchers is the comparison of United States, Russian, and French Nd-glass lasers. This topic was discussed at most of the laboratories. Much more is known about the French Nd-glass than about the Soviet Nd-glass. The French Nd-glass is selected by coring from large melts (one meter in diameter by 0.31 m thick), while the U.S. Nd-glass is drawn from much smaller melts. Most agree that the U.S. Nd-glass is inferior to both the French and the Russian Nd-glass. The reasons for this are in part financial. It is estimated that the French Nd-glass laser research effort is funded at twice the United States rate. But, money alone does not solve problems. Based on the scant information the writer could obtain, the organization of the French research differs substantially from the organization in the U.S. The French effort is directed and coordinated more strongly than the U.S. It is certain that the total number of French laser research laboratories is less than that for the U.S. There is only one French manufacturer of high power pulsed Nd-glass lasers; one French supplier of Nd-glass rods and one major contract granting office. Such reasons as the above are most speculative. However, the writer does know that in one instance the French effort on materials research is more sophisticated than that of the U.S. When damage tracks occur in glass or when surface damage (pits) occur, the defects emit light. The researchers (J. Ernest, et al.) have studied the spectral content of such emissions with time. Unfortunately, these experiments are not reported in the open literature and the quantitative results of the experiments are not available to the writer. Except for NBS the writer has not been able to locate one group in the U.S. which has or plans similar studies on either Nd-glass lasers in the 30 nanosecond pulse range. This is one way in which

the changes in the electronic energy levels of either the bulk or surface may be studied as a function of doping (e.g.,  $TiO_2$ ) or as a function of surface treatment (etching and ion exchange). When electrons lie in deeper states (are bound more tightly) larger electric fields are necessary before the electron can be raised to a conduction band or free electron state. Conduction or free electrons may cause damage more readily by avalanching than may tightly bound electrons.

As the writer travelled from one laboratory to the other he began to realize that a lack of communication among laser researchers in high power pulsed lasers exists. If one assumes that the development of high power pulsed lasers is a national undertaking, then open and frank discussions of one another's efforts and problems are most essential. The common means of communication is the published and open literature. This is a medium in which researchers are understandably reluctant to state their unsolved problems. But these must be made known to others if the device development is to proceed with a minimum of time and effort. But the general rule was that of isolation. It is true that pico-second, nano-second, and micro-second pulses differ, but much knowledge in one time domain can be applied to other time domains. For example, flash lamp designs for the pico-second and nano-second time domains have many common characteristics. Yet, the practical advantages and disadvantages of helical lamps, axial lamps, (parallel to the laser axis) and perpendicular lamps (perpendicular to the laser axis) are not widely known among the laboratories. Workers in one time domain tend to isolate themselves from workers in other time domains. One result of this lack of communication becomes apparent at meetings such as the ASTM Symposium on Damage in Laser Glass, which was held on 20 June 1969 at the National Bureau of Standards (Boulder,

Colorado). Each invited paper was almost completely self-contained and related little to the other papers presented at the Symposium. Laboratories associated with universities tend to communicate more freely than those associated with industries and the Government. This same ASTM symposium also illustrates the clinical nature of the recent studies on damage and degradation. That is, the results from laser "a" at laboratory A are frequently unique and are most difficult to compare with the results from laser "b" at laboratory B. The difficulty lies mostly in obtaining the same reproducible pulses of known spatial and temporal behavior from different lasers. However, improved inter-laboratory communication could alleviate the situation.

One problem concerns the incomplete reporting of results in the literature and the incomplete nature of the research. Two striking examples exist. First, it has been reported that etching the end surfaces of Nd-glass rods with hydrofluoric acid increases the threshold for surface damage by about a factor of three. But, the surfaces after treatment are deteriorated and are not of good optical quality for laser materials. Second, doping ruby rods with  $TiO_2$  increases the internal damage threshold substantially. Some reports indicate that an order of magnitude increase obtains. Again, the rods after treatment are no longer suitable for use as laser rods. Even though these effects have been known for at least a year, no one in the United States, to the writer's knowledge, is studying the possible mechanisms, chemistry or physics, responsible for these increased thresholds or how to increase the threshold without degrading the optical and laser qualities.

The empirical approach to laser materials research has been adequate in the past. That is, the damage or degradation to laser materials has been circumvented by equipment

design, by using another material, or by simply asking for lower laser power. When a material was found to be superior, little effort was devoted to understanding the chemistry and or physics of why it brought about an improvement. The writer feels that now the empirical approach to the materials problem must be complemented by a fundamental materials research program which is coordinated closely with the needs of those who use specialized lasers.

Finally, the damage to Nd-glass laser rods remains a confusing area. It is rare that more than two researchers from different laboratories agree with one another. Definitive experiments which permit reasonable and confident interpretation of the damage results have not been performed yet. Most damage studies use photographs exposed for times much greater than the pulse width. More useful information obtains if the damage tracks are photographed as a function of time on a time scale comparable to the pulse width. One then acquires information on the rate of growth of the track, direction of growth of the track, and the time at which the damage site first appears. These quantities are essential when one attempts to suggest the dominant mechanism which is responsible for the damage site or track. Present damage studies do not include such details. The writer is aware of only one case in which future plans include them. He feels that only by knowing the spatial and temporal shape of the laser pulse, by examining the spectral emission, with time and by taking photographs as the damage develops can one hope to reduce the present extent of confusion and lack of consensus of opinion.

#### Technical Information:

Prof. E. C. Crittenden and his students have generated acoustic waves at 500 MHz by the electrostrictive beating of two coherent ruby laser pulses in dense lead glass. They expect to obtain frequencies as high as 50 GHz. The gener-

ated acoustic waves had an amplitude greater than that expected from quantum considerations; but still not great enough to fracture the dense lead glass. Some of the pulses fractured the dense lead glass. They say that the fractures might have been due to inclusions and not due to the absorption of acoustic waves. If they had better knowledge about the change of index of refraction with temperature and with stress they would have had fewer design problems with their experiment. In addition, they also observed surface damage pits on the ruby laser rod after a few thousand pulses. Due to thermal drifting, the pulse repetition rate never exceeded one pulse every twenty minutes.

Prof. S. Harris has five major projects. Two or more graduate students work on each project. Four projects develop non-linear optical devices. One of the projects studies the materials problems encountered by the other four projects. Dr. R. Byers heads the materials project. They have encountered many damage and degradation problems with the following non-linear materials;  $\text{LiNbO}_3$ ,  $\text{Ba}_2\text{NaNb}_5\text{O}_{15}$ ,  $\text{KH}_2\text{PO}_4$ ,  $\text{HIO}_3$ ,  $\text{LiIO}_3$ ,  $\text{CdS}$ ,  $\text{CdSe}$ ,  $\text{CsPbCl}_3$ ,  $\text{LiTaO}_3$ , and  $\text{PbMoO}_4$ . In many cases only a factor of ten exists between the threshold energy density for the non-linear mechanism to occur and the threshold energy density for surface burns and internal tracks. One tries in designing devices to optimize the figure of merit ( $D^2/n^3$ ) and the second harmonic generation (SHG) power against the burn or damage threshold. The index of refraction is  $n$  and the non-linearity (non-linear susceptibility) is  $D$ . The bulk optical properties of the above materials ( $dn/d\omega$ ,  $dn/dT$ , birefringence, and the photo-elastic coefficients) have not been measured well in any of the above materials. These quantities are needed for designing non-linear optical devices. The researchers consequently must do these measurements themselves. They commonly employ Q-switched pulses which are tens of nano-



seconds in length and which have power densities from 10 to 100 MW/cm<sup>2</sup>. In addition, in many cases they have had to grow the crystals themselves. They say and their output shows that one cannot develop devices without high quality optical materials. They experience considerable burn damage in the complex dielectric and metallic coatings for anti-reflection elements and mirrors. They also find that damage is less likely to occur when the laser mode is closely controlled and consistently reproducible. Prof. Pantell says that materials are the main limitations in non-linear optic studies. There is a need to gather data on testing techniques, to enumerate the data on non-linear materials and to keep the data current on materials from the far infrared to the ultra-violet.

Dr. J. Swain's group designs high power pulsed lasers to study high density and high temperature plasmas and shock waves. They seek to obtain as much energy as possible in nanosecond and picosecond pulses. In order to circumvent the damage problem in ruby, they previously brought the beams from 12 ruby lasers to the surface of a sphere and focused them to a central point with lenses (5 cm. focal length). They now are building Nd-glass disc lasers. They plan to have a 5 element Nd-glass disc (12.5 cm. diameter by 1.25 cm. thick) laser in operation by August 1969. A 15 element Nd-glass disc (12.5 cm. diameter by 1.25 cm. thick) laser, which has the mirrors about 55m. from the nine-pass amplifier, is being constructed. The feasibility of pumping a 39 cm. diameter disc by a shock wave excited flash is being examined. Conventional flash lamps are not efficient optical pumps for this size disc. The 5 element disc laser contains axial flash lamps and is expected to produce a 10 nanosecond pulse with an energy of about 10 joules. Power levels of the order of 100 GW are expected by focusing the beam down to a 10<sup>-2</sup> cm. spot. The 15 element disc laser contains perpendicular flash lamps and is expected to

produce 1000 joules per  $60 \text{ cm}^2$  in a 3 nanosecond pulse. They estimate that the 39 cm. disc laser will produce pulses having 10,000 joules in a tens of nanosecond pulse, if they can find an efficient way to transfer stored energy to create a uniform population inversion. Studies to bring about a population inversion by chemical energy (chemical reactions) have also been conducted. The source of most problems and limitations associated with high power and high radiance laser rods is due to optical pumping through the cylindrical surface. This Livermore group does not seek high repetition rates and hence is not concerned with excessive heating problems. The above disc lasers are face pumped. The discs are centimeters apart and set at Brewster angles with respect to one another. The optical absorption is an asset here because it means a large energy storage capability. Face pumping also leads to a more radially uniform population inversion. The internal damage due to self focusing is lessened when discs of a thickness less than the critical self-focusing distance are used. They use these large aperture disc systems to reduce thermal distortion, improve pumping efficiency, and to have a more radially uniform population inversion. Their major damage problem arises from surface damage pits. Because no one else has examined the problem to their satisfaction they have undertaken an empirical surface damage study. Even though treating the surface with hydrofluoric acid increases the surface damage threshold by a factor of three, they find that the optical quality becomes unsuitable for laser applications.

Dr. Winston and Dr. C. Giuliano plan to cooperate and to collaborate very closely with Dr. M. Stickley and Dr. E. Bliss of the Air Force Cambridge Research Laboratory (AFCRL). They will study damage to ruby and sapphire samples with very slightly converging beams (long focal length

compared to sample size). The Hughes group will examine surface and internal damage thresholds with 3 to 100 nanosecond pulses and the AFCRL group will examine the same with 0.1 and 100 nanosecond pulses. They will use single modes and know the temporal properties of the beam. They plan to examine the ruby damage tracks and cleavage faces as they develop in time with a streak camera (image converter camera). A possibility exists that they also will examine the tracks and cleavage faces with an electron microscope. A debate exists as to whether the threshold for surface damage in ruby is greater or less than the internal damage threshold in ruby. They believe that Czochralski crystals may have more contaminants than the Verneuil crystals but that the optical qualities of Czochralski crystals are better than those of the Verneuil crystals. In order to compare results at laboratory A with those at laboratory B, they assert that one must use well-behaved, non-fluctuating beams in both space and time.

Dr. A. Keig directs the characterization of crystals grown at Union Carbide. The Electronics Division of Union Carbide (San Diego) is an important supplier of Czochralski grown ruby crystals in the United States. Dr. L. Rothrock (Union Carbide) says that electrostrictive self-focusing has been observed in white sapphire ( $\text{Al}_2\text{O}_3$ ) but not in ruby. The debate persists as to whether "yellow" ruby is still a problem with recent (less than one year) Union Carbide grown crystals. One side says that the problem is most likely related to the impurity content and the other says that it is related to changes in the volume of chromium ions. On the other hand, his group observes that bulk damage in ruby is power-density-dependent and suggests that multiphoton absorption occurs or that other impurities, which do not play a role in the "yellow" ruby debate, absorb energy and modify the energy levels. It is also their opinion that the

Schulz-Wei method is as good as the Laue-x-ray-back-scattering method to study the wander of the c-axis. The most recently grown ruby crystals are so good now that the c-axis orientations differ by less than a minute. New techniques are needed to test the most recent ruby crystals because present techniques are not sensitive enough. The Nd-YAG crystals have many more problems than ruby and Nd-glass. They also have a program to improve the optical quality of Nd-YAG. During the past year they have reduced the average number of interference fringes across the face of a rod in an interferometer from 2 for a .64cm x 5.08cm rod to 1.5 for a 64cm x 7.62cm rod.

Dr. G. Gobeli and Dr. E. Jones have constructed a Nd-glass laser which emits 75 joules in a one to two picosecond pulse. The pulse length is expressed in terms of the two photon fluorescence experiments. The interpretation of the two photon fluorescence experiments is controversial and is not the subject of their research. They built this laser as a tool with which to study solid state physics and do not consider the continual development of high power lasers to be their major endeavor. They hope to generate thermonuclear neutrons by focusing the laser on a solid LiD surface. They expect to obtain power densities of  $10^{20}$  watts/cm<sup>2</sup> over an area  $10^{-6}$  cm<sup>2</sup>. The spatial and temporal properties of the picosecond pulses are of secondary interest to them. Their major damage problem centers on the metallic and dielectric coatings of the 100 percent mirrors. The laser rod damage occurs much less frequently. Most rods last thousands of pulses before replacement due to damage is necessary. But, most mirrors last only 20 to 50 pulses before a "burn" spot develops and the mirror must be replaced. The 100 percent reflection coatings provided by all manufacturers are universally of a poor quality for their purposes. They have found that rods from the same melt have widely different

damage characteristics. One rod will last perhaps only three pulses: while another rod from the same melt will last 1000 pulses. Removing such differences from supposedly identical laser rods is more important to them than debating about which Nd-glass rod supplier produces the most superior product. Damage to mirrors and rods sometimes occurs in their system when the (always present but hopefully small) diffuse scattering from an optical surface causes prelasing in high gain regions. A significant difference exists between a single picosecond pulse and a train of several picosecond pulses. The latter often produces plate-like damage sites which are very similar to the damage sites produced by Q-switched nanosecond pulses in plastics. They plan to study damage in all of their laser components to enable them to accomplish their primary mission (to make a tool for solid state physics studies). They will attempt to understand the propagation characteristics of high power laser beams in transparent materials such as silica, sapphire, and glass. The lack of sufficient controls on damage experiments to date make inter-laboratory comparisons very hazardous undertakings. The experimental techniques and the spatial and temporal properties of the laser pulses in a given laboratory differ markedly from those in other laboratories.

Capt. A. Abela is familiar with the Nd-glass damage problems encountered by the Kirtland Air Force Weapons Laboratory researchers. Due to limitations on funds and personnel, other projects have a higher priority than the glass damage studies. They recognize however the importance of damage studies. They do plan some damage studies which will be limited probably to visual observations and which will be undertaken only to the extent necessary to accomplish their mission. Their efforts are directed towards the application of Q-switched pulses which are 30 to 80 nanoseconds in length. They initially seek 50 joules per pulse, 5 pulses per second, and 5 cm. diameter beam. Their studies will be

mainly with collimated beams. They would like a figure of merit to be provided for each type of Nd-glass. That is, an evaluation based upon lasing efficiency, laser threshold, beam divergence, signal gain, and rod distortion during pumping. They need specific glasses around which they will design their systems. He also agrees with others that comparing data at one location with that from another location is difficult and provides little additional understanding. They have a slab (disc) laser designed with the discs very close together. Only close examination reveals that the laser "rod" is composed of many discs. The laser is pumped through the cylindrical surface. They employ the disc system mainly to circumvent the cooling problem of a conventional laser rod. Their needs and applications are in the realm of limited access information.

Prof. D. Edwards and his students are sponsored in part by the Air Force Cambridge Research Laboratories to carry out laser damage studies in transparent materials. His group examines the details of the Raman spectra before damage occurs, near the damage sites after it occurs, and as a function of uniaxial stress. They have studied most thoroughly quartz, but also have made preliminary examinations on ruby, sapphire, salt (NaCl) and glass. They measure the line position, line width, and line intensity. The latter two quantities relate to the anharmonic parts of the lattice potential. The above quantities are used first to characterize the undamaged or stress-free materials. After characterization by the Raman spectra they have two approaches. First, the material is damaged by a laser beam and then examined a second time near the damage sites by Raman spectroscopy. The amount by which the above quantities change may suggest possible mechanisms for the damage. Second, a uniaxial stress is applied in the range of stress which they estimate from a laser beam without specifying

the exact nature of the electromagnetic wave-lattice coupling. The above quantities are studied as a function of the applied uniaxial stress. They expect to be able to make some correlations between how the line width changes with stress and the damage thresholds. He observes that the Russians have a substantially greater effort on damage in resin materials (plastics) by lasers. He also remarks that past successes have been accomplished without a sound materials effort; but now materials research is going to be essential for further achievements.

Because some of the foregoing technical information also was presented at the ASTM Nd-glass Symposium (20 June 1969, Boulder, Colorado) and because the Symposium proceedings are to be distributed, the writer feels that it is redundant to include a summary of the ASTM Symposium in this trip report.





# NBS TECHNICAL PUBLICATIONS

## PERIODICALS

**JOURNAL OF RESEARCH** reports National Bureau of Standards research and development in physics, mathematics, chemistry, and engineering. Comprehensive scientific papers give complete details of the work, including laboratory data, experimental procedures, and theoretical and mathematical analyses. Illustrated with photographs, drawings, and charts.

*Published in three sections, available separately:*

### ● Physics and Chemistry

Papers of interest primarily to scientists working in these fields. This section covers a broad range of physical and chemical research, with major emphasis on standards of physical measurement, fundamental constants, and properties of matter. Issued six times a year. Annual subscription: Domestic, \$9.50; foreign, \$11.75\*.

### ● Mathematical Sciences

Studies and compilations designed mainly for the mathematician and theoretical physicist. Topics in mathematical statistics, theory of experiment; design, numerical analysis, theoretical physics and chemistry, logical design and programming of computers and computer systems. Short numerical tables. Issued quarterly. Annual subscription: Domestic, \$5.00; foreign, \$6.25\*.

### ● Engineering and Instrumentation

Reporting results of interest chiefly to the engineer and the applied scientist. This section includes many of the new developments in instrumentation resulting from the Bureau's work in physical measurement, data processing, and development of test methods. It will also cover some of the work in acoustics, applied mechanics, building research, and cryogenic engineering. Issued quarterly. Annual subscription: Domestic, \$5.00; foreign, \$6.25\*.

## TECHNICAL NEWS BULLETIN

The best single source of information concerning the Bureau's research, developmental, cooperative and publication activities, this monthly publication is designed for the industry-oriented individual whose daily work involves intimate contact with science and technology—for *engineers, chemists, physicists, research managers, product-development managers, and company executives*. Annual subscription: Domestic, \$3.00; foreign, \$4.00\*.

\* Difference in price is due to extra cost of foreign mailing.

## NONPERIODICALS

**Applied Mathematics Series.** Mathematical tables, manuals, and studies.

**Building Science Series.** Research results, test methods, and performance criteria of building materials, components, systems, and structures.

**Handbooks.** Recommended codes of engineering and industrial practice (including safety codes) developed in cooperation with interested industries, professional organizations, and regulatory bodies.

**Special Publications.** Proceedings of NBS conferences, bibliographies, annual reports, wall charts, pamphlets, etc.

**Monographs.** Major contributions to the technical literature on various subjects related to the Bureau's scientific and technical activities.

**National Standard Reference Data Series.** NSRDS provides quantitative data on the physical and chemical properties of materials, compiled from the world's literature and critically evaluated.

**Product Standards.** Provide requirements for sizes, types, quality and methods for testing various industrial products. These standards are developed cooperatively with interested Government and industry groups and provide the basis for common understanding of product characteristics for both buyers and sellers. Their use is voluntary.

**Technical Notes.** This series consists of communications and reports (covering both other agency and NBS-sponsored work) of limited or transitory interest.

**Federal Information Processing Standards Publications.** This series is the official publication within the Federal Government for information on standards adopted and promulgated under the Public Law 89-306, and Bureau of the Budget Circular A-86 entitled, Standardization of Data Elements and Codes in Data Systems.

## CLEARINGHOUSE

The Clearinghouse for Federal Scientific and Technical Information, operated by NBS, supplies unclassified information related to Government-generated science and technology in defense, space, atomic energy, and other national programs. For further information on Clearinghouse services, write:

Clearinghouse  
U.S. Department of Commerce  
Springfield, Virginia 22151

Order NBS publications from: Superintendent of Documents  
Government Printing Office  
Washington, D.C. 20402

U.S. DEPARTMENT OF COMMERCE  
WASHINGTON, D.C. 20230

OFFICIAL BUSINESS



POSTAGE AND FEES PAID  
U.S. DEPARTMENT OF COMMERCE

---